International Journal of Concrete Structures and Materials

RESEARCH

Open Access

Evaluation of Mechanical Properties and Water Resistance Performance of Concrete Modified with Graphene Nanoplatelets (GNP)

Leidys Johana Jaramillo[1] and Robin Kalfat[1*]

Abstract

Nano materials made from graphene have emerged as highly effective additives that can significantly improve the engineering properties of cement-based composites. This research investigated the impact of adding graphene nanoplatelets (GNP) on the performance of concrete, using both sonicated and non-sonicated GNP dispersions. The study evaluated fresh concrete properties through slump tests, and mechanical characteristics were analyzed at 7, 14, and 28 days by conducting tests for compressive, flexural, and tensile strength. Homogeneity was assessed using ultrasonic pulse velocity (UPV), while durability was evaluated by examining water absorption (Ai), apparent volume of permeable voids (AVPV), and sorptivity. Furthermore, scanning electron microscopy (SEM) and energy dispersive spectrometry (EDS) were employed to study how GNP affected the microstructure of concrete. The research found that the most significant improvements in engineering properties occurred when sonicated GNP dispersions were added at a concentration of 0.25 wt%. This addition resulted in enhancements of compressive, flexural, and tensile strengths by 20.8%, 10.5%, and 11.4%, respectively, at 28 days. UPV also improved by 12.9% at the same GNP concentration. Furthermore, Ai, AVPV, initial sorptivity, and secondary sorptivity decreased by 28.3%, 26.3%, 22%, and 27%, respectively, at 28 days. Microscopic analysis indicated that GNP contributed to reinforcing the microstructure of concrete through nucleation and filling effects, thereby enhancing the material's overall engineering performance.

Keywords Graphene nanoplatelets (GNP), Concrete, Sonication, Cement, Sorptivity, SEM, EDS, Durability, UPV, Water absorption, Permeability

1 Introduction

Over the past 40 years, global cement production has increased nearly fourfold, leading to significant environmental consequences (Andrew, 2019). Cement manufacturing releases a substantial amount of carbon dioxide (CO_2) into the atmosphere, contributing approximately 8% of global carbon emissions (Ali et al., 2011; Andrew, 2019), thereby ranking as one of the largest sources of man-made CO_2 emissions worldwide (Barcelo et al., 2014). Consequently, it is crucial to develop and implement innovative strategies aimed at reducing the carbon footprint associated with concrete. Proposed approaches to mitigate emissions from cement production include: i) carbon capture and storage (CCS) (Bandilla, 2020), ii) enhancing the energy efficiency of cement manufacturing processes (Madlool et al., 2013), iii) substituting cement partially or entirely with alternative materials, such as fly ash and blast-furnace slag (Lovecchio et al., 2020), or incorporating carbon nanomaterials, such as graphene oxide (GO), graphene nanoplatelets (GNP), reduced graphene oxide (rGO) (Babak et al., 2014), graphene quantum dots (GQDs) (Win et al., 2024a, 2024b), and iv)

Journal information: ISSN 1976-0485/eISSN 2234-1315.

*Correspondence:
Robin Kalfat
rkalfat@swin.edu.au
[1] School of Engineering, Swinburne University of Technology, Hawthorn, VIC 3122, Australia

integrating industrial by-products into concrete (Papayianni & Anastasiou, 2010).

Additive carbon nanomaterials such as GO, GNP, and rGO have been proposed as new alternatives to partially replace cement while achieving the same strength and greater durability. Graphene oxide (GO) is typically synthesized from graphite through chemical oxidation, involving oxygen functional groups, such as epoxide, carbonyl, carboxyl, and hydroxyl. These groups alter the crystal structure and properties of graphite, making GO advantageous for enhancing cement composites. Due to its hydrophilic nature conferred by these oxygen groups, GO easily disperses in aqueous solutions. This property gives GO amphiphilic characteristics akin to surfactants, making it useful as a dispersing agent for GNP in water-based environments (Babak et al., 2014).

Despite these benefits, GO is constrained by its high production costs and process complexities and as an alternative, multilayer GNP are often preferred in practical applications. GNP can be more straightforwardly derived from graphite through mechanical exfoliation, which is more economically viable compared to the chemical exfoliation methods required for production of GO. Both GO and GNP derive from graphene and boast exceptional mechanical properties, but GNP are generally considered stronger and more stable in applications. As a result of their outstanding properties, GNP have also become an innovative form of nano-reinforcement used in concrete for a wide range of applications. One graphene sheet exhibits impressive properties such as tensile strength of up to 120 GPa (Papayianni & Anastasiou, 2010), young's modulus of around 1 TPa (Chen et al., 2020), electrical conductivity of 1 S/m, and thermal conductivity of ~ 2000–4000 W/K at room temperature (Papanikolaou et al., 2021a).

GNP can enhance the mechanical properties of concrete but typically lead to decreased workability. Chen et al. (Chen et al., 2019) investigated the impact of GNP on concrete's compressive strength and workability and observed that as the GNP content increased to 0.4 wt%, the slump of the concrete decreased from 70 mm to 57 mm. This reduction in slump was directly proportional to the increased GNP content, attributed to the high surface area of the GNP. Examining various GNP concentrations, the study also explored GNP concentrations ranging from 0.02 to 0.3 wt% in concrete and reported increases in compressive strength of: 18%, 61%, 22.4%, 19.78%, 8.84%, and 1.42%, respectively. The study concluded that 0.05 wt% GNP offered optimal mechanical benefits, as higher concentrations led to agglomeration and heterogeneous mixtures, limiting strength gains. However, there was no information provided regarding the effects of GNP on concrete flexural strength, tensile strength, homogeneity, and water resistance.

Du et al. (Du et al., 2016) investigated the impact of adding GNP ranging from 0.0 wt% to 2.5 wt% on the compressive and splitting tensile strength of mortar specimens at 28 days. The study concluded that GNP did not enhance the compressive strength of the specimens, attributing this to minimal changes in mortar porosity after GNP introduction. Consequently, no significant improvements were observed in the mechanical properties of concrete. Regarding transport properties, the study found that adding 1.5% GNP reduced water penetration depth, chloride diffusion, and migration coefficients by 80%, 80%, and 37%, respectively. Du et al. (Du et al., 2016) suggested that GNP increased tortuosity in mortar, thereby enhancing resistance to water infiltration. However, they did not provide information on how GNP influenced the workability and homogeneity of mortar specimens. Their research primarily focused on evaluating GNP's effect on chloride ion penetration as an indicator of concrete durability, but did not explore critical parameters, such as water absorption (Ai), apparent volume of permeable voids (AVPV), and initial and secondary sorptivity. Furthermore, Papanikolaou et al. (2021) (Papanikolaou et al., 2021a) recently reported a 75% increase in viscosity with the addition of only 0.1 wt% GNP to cement paste compared to conventional materials. However, their study did not investigate the influence of GNP on workability, mechanical properties, or water resistance.

The impact of GNP on the strength properties of cementitious materials is closely tied to the quantity of GNP added. Wang et al. (Wang et al., 2016) assessed cement paste strength characteristics with 0.05 wt% GNP over 3, 7, 14, and 28 days, observing increases in both compressive and flexural strength at each interval. For instance, at 28 days, compressive strength improved by 3% and flexural strength by 16.8%. In another study, Chen et al. (Chen et al., 2023) noted an 11.6% increase in flexural strength with 0.02 wt% GNP.

In recent research, Jiang et al. (Jiang et al., 2021) found that adding 0.025 wt% GNP yielded a 17% increase in compressive strength after 28 days. Similarly, Arslan et al. (Arslan et al., 2022) determined 0.14 wt% as the optimal GNP concentration for ultra-high strength concrete. In mortar, Polverino et al. (Polverino et al., 2022) reported a 29% enhancement in compressive strength with 0.15 wt% GNP and 24% with 0.1 wt% GNP.

Conversely, Adhikary et al. (Adhikary et al., 2022) observed substantial increases of up to 43% in compressive strength and 42% in flexural strength with 0.25 wt% GNP. However, other studies have shown mixed results: Du & Pang (Du & Pang, 2015) noted slight increases in compressive strength with 5 wt% GNP in cement mortar but decreases at higher concentrations. Similarly, Jiang et al. (Jiang et al., 2020) reported enhanced tensile strength with 0.1 wt% GNP in mortar, whereas Alwash et al. (Alwash et al., 2021) and Shuang et al. (Shuang et al., 2022) found that agglomeration of GNP led to reduced mechanical properties in cement paste.

The reinforcing effects of GNP in calcium aluminate cement (CAC) composites have recently been explored by Win et al. (Win et al., 2023) who evaluated the synergistic effects of GNP and fly ash (FA) in CAC composites. The study also investigated the partial replacement of CAC with FA to enhance sustainability and reduce material costs in GNP–CAC composites. The study found that the incorporation of FA and GNP into CAC composites positively impacted their strength properties. The optimal mix involved replacing 20% of FA and adding 0.3% of GNP in CAC composites. Results demonstrated that this combination significantly increased compressive, splitting tensile, and flexural strengths at 28 days by approximately 57.2%, 35.5%, and 21.7%, respectively.

The strength and durability of concrete depend on its consistency, uniformity, and overall quality. Assessing the uniformity and integrity of concrete often involves using an ultrasonic pulse velocity (UPV) test. This non-destructive method has been widely employed in the construction industry for over 60 years (Malhotra & Carino, 2004) to gauge concrete's integrity and uniformity, offering crucial insights into its strength and consistency. In laboratory settings, UPV has been utilized to evaluate how nanomaterials influence the uniformity of cement composites (Mohammed et al., 2017; Rajesh & Narendra Kumar, 2022; Zeng et al., 2021), demonstrating that these materials can enhance concrete quality by improving its consistency and uniform distribution. Despite these advancements, there is limited research on the specific effects of GNP on the homogeneity, uniformity, and overall quality of concrete. Given UPV's effectiveness in providing initial insights into these aspects, this study utilized UPV to investigate the impact of GNP on concrete.

Although incorporating GNP into concrete can enhance mechanical strength and durability of structures, previous studies on their impact on workability, mechanical properties, and water resistance of concrete are limited and disjointed. Moreover, few studies have explored the effects of non-sonicated and sonicated GNP dispersions on concrete's engineering properties across different ages. Previous research predominantly focused on either non-sonicated or sonicated GNP dispersions in concrete. Given these gaps, further investigation into the effects of GNP on concrete properties is crucial for its effective application in buildings and infrastructure, motivating this study. This research evaluates the influence of non-sonicated and sonicated GNP dispersions on the mechanical properties, uniformity, and water resistance of concrete specimens at 7, 14, and 28 days. In addition, it examines the impact of GNP on the microstructure of concrete specimens through Scanning Electron Microscopy (SEM) and Energy Dispersive Spectroscopy (EDS). The study aims to achieve several objectives: (1) analyze the effects of GNP on compressive, flexural, and tensile strength of concrete specimens over time; (2) determine the optimal superplasticizer (SP) content to mitigate GNP's impact on fresh concrete properties and mix workability; (3) assess GNP's influence on water absorption (Ai), apparent volume of permeable voids (AVPV), water sorptivity, and UPV values of concrete specimens at different ages; (4) conduct microstructural analysis of GNP-incorporated concrete using SEM and EDS; and (5) evaluate the reduction in cement consumption necessary to achieve a specific strength class in GNP-enhanced concrete specimens.

This research significantly contributed to the academic community by offering fresh perspectives on the influence of non-sonicated and sonicated GNP dispersions on the strength, durability, and microstructure of concrete. The findings of this study offered solutions to mitigate the environmental footprint of concrete by leveraging GNP to produce high-strength concrete using less cement while improving durability. This enhanced durability could potentially lead to decreased carbon emissions linked to the upkeep, repair, and renovation of concrete structures.

2 Materials and Methods

2.1 Materials

All samples tested in this study were prepared using Ordinary Portland Cement (OPC) as the primary binding material. The OPC used fully complied with the requirements for general purpose cement (Type GP) as specified in AS3972 (AS, 2010), and included both coarse and fine aggregates. The particle size distribution of these aggregates is illustrated in Fig. 1. Coarse aggregates, consisting of crushed granite with a maximum particle size of 20 mm, were utilized. Fine aggregates were sourced from washed sand. The physical properties of both coarse and fine aggregates were determined following ASTM standards C127 (ASTM, 2007a) and C128 (ASTM, 2007b). The densities of 7 mm, 14 mm, and 20 mm aggregates, as well as washed sand, were measured as 2573 kg/m^3, 2563 kg/m^3, 2224 kg/m^3, and 2004 kg/m^3, respectively. The absorption rates for these aggregates were found to be 2.22%, 1.59%, 1.88%, and 5.34%, respectively. For the concrete mixtures, a polycarboxylate-based superplasticizer (SP) (ViscoCrete 5–500) supplied by Sika was used. An

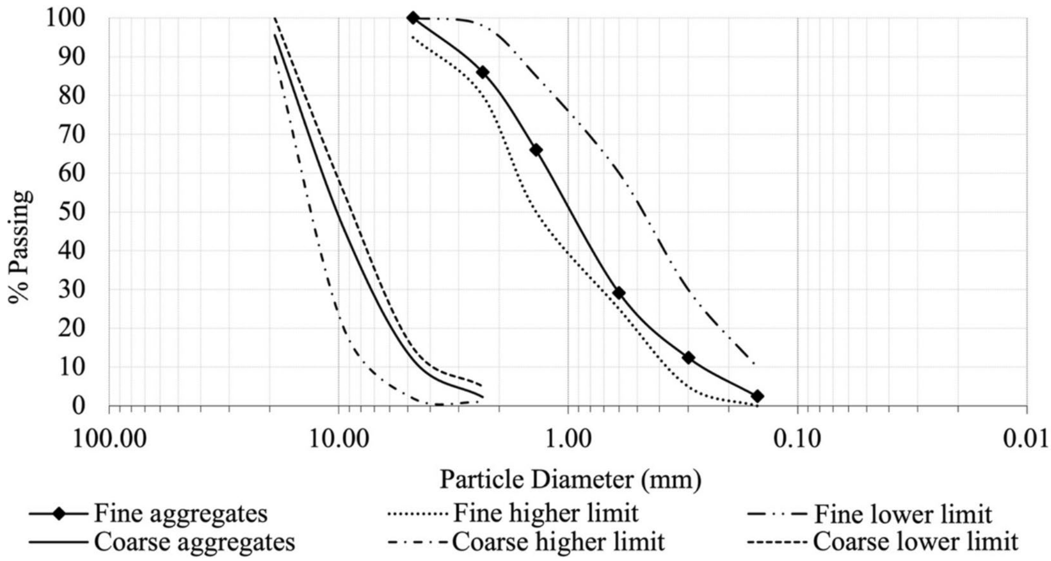

Fig. 1 Particle size distribution of fine and coarse aggregates

Table 1 Physical properties and elemental composition of solid GNP

Flake size (μm)	Thickness (nm)	Surface area (m^2/g)	Density (g/cm^3)	Carbon (%)	Oxygen (%)	Impurities (%)
2–6	< 3	536	0.02	> 99.4	< 0.5	< 0.1

aqueous graphene paste consisting of 32% pure graphene and 68% water was supplied by APNTeK. Table 1 outlines the physical characteristics and chemical composition of the GNP used in this study.

SEM images of the GNP used in this study were taken from multiple locations to ensure their representativeness, and were published in Jaramillo & Kalfat (Jaramillo & Kalfat, 2023). These images revealed that GNP exhibit a wrinkled and folded morphology, consistent with prior research indicating that wrinkles and folds are characteristic features of GNP. In addition, the images show large clusters of graphene nanosheets formed by the agglomeration of individual sheets. Consequently, the average length of GNP varied, measuring approximately 14 μm on average.

2.2 Mixing Methods

This study was conducted in four experimental phases to achieve the goals outlined above. A concise and organized description of these phases is presented below:

(a) Phase I: Optimum amount of SP

Since it was observed that the addition of GNP reduced slump values of fresh concrete mixes below acceptable limits, the first phase of the study was focused on improving the workability of the developed mixes. To achieve this aim, two wet methods for dispersion of GNP in water were used. The first wet dispersion method consisted of the preparation of non-sonicated GNP dispersion containing super plasticizer (SP) which were mixed together using a drill. The second wet dispersion method involved the preparation of sonicated GNP dispersion containing SP. In second mixing method, the GNP dispersion was first mixed in water solution using a drill and then by ultrasonic probe. To determine the optimal SP content, various dispersions of GNP were prepared while keeping the concentration of GNP constant. For the preparation of each GNP dispersion, the amount of SP was varied. After preparation, each GNP dispersion was added to the concrete raw materials (cement, fine and coarse aggregates), mixed and the slump values of the fresh concrete mix was measured. The amount of SP added was increased gradually until the slump value was similar to that of the fresh control mix. The same procedure was used to calculate the optimum content of SP for both non-sonicated and sonicated GNP dispersion.

(b) Phase II: Mechanical properties

In the second phase of this study, we selected the non-sonicated and sonicated GNP dispersion prepared with the optimal amount of SP discovered in phase 1. The effect of non-sonicated and sonicated GNP dispersions on strength of concrete specimens was assessed by determining compressive, tensile and flexural strength at 7, 14 and 28 days, respectively.

(c) Phase III: Homogeneity and water resistance of concrete

In the third phase of this investigation, the durability aspects of the mixes in terms of water resistance and homogeneity of concrete were explored. After preparation of non-sonicated and sonicated GNP dispersion, the dispersions of GNP were added to the cement and aggregates and concrete specimens were cast and cured for 7, 14 and 28 days, respectively. An analysis of the influence of both GNP dispersions on the homogeneity and uniformity of concrete was studied using the UPV test. The results and discussion are presented in Sect.UPV assessment. Next, the impact of both GNP dispersions on Ai, AVPV and sorptivity was examined.

(d) Phase IV: Microstructure analysis

In the fourth phase of this study, microstructure analysis of plain concrete and concrete prepared using GNP was conducted for D2-E which had the highest engineering performance.

(e) Phase V: Cement consumption reduction

In the fifth phase, an evaluation of the reduction of the amount of cement required to prepare concrete with GNP was conducted. For this purpose, an assessment of the cement consumption of all concrete mixes was conducted using binder intensity (bi) index.

2.2.1 Preparation of GNP Dispersion for Phase 1

In this study, GNP dispersion was mixed using either a drill for 5 min for group 1 specimens or a combination of drill for 5 min followed by ultrasonic probe for 20 min for samples in group 2. From an earlier phase of the research program (Jaramillo & Kalfat, 2023), 0.25wt% GNP was found to be the optimal concentration of nanomaterial which resulted in the highest compressive strength. As a result, the GNP content was fixed at 0.25wt% for all the mixes used in this phase of the study and only the SP concentration was varied. The amount of SP explored were 0.2, 0.4, 0.6, 0.8, 0.9, and 1.0 wt%.

For the sonication treatment, the following parameters were used: (1) power output of 500 W; (2) probe frequency of 20 kHz; and (3) a horn diameter of 20 mm. The sonication treatment was conducted at intervals of 2.5 min which consisted of continuous sonication for 2.5 min, followed by 15 s rest followed by another 2.5 min of sonication until the total sonication time had elapsed. This was necessary to avoid overheating of the sample. To prevent GNP segregation during the 15 s rest period, the dispersion was mixed using a drill mixer during this time prior to the next sonication interval. A schematic representation of the two groups of GNP dispersion is displayed in Fig. 2.

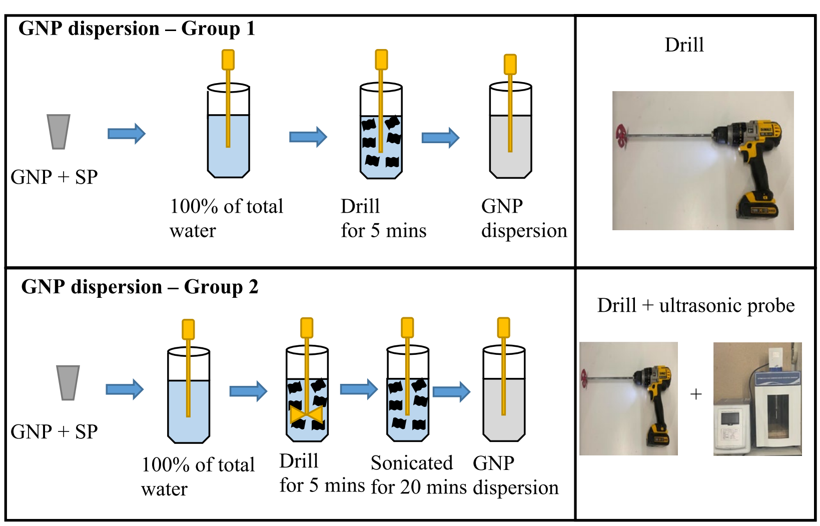

Fig. 2 A schematic representation of wet dispersion mixing methods used for the preparation of GNP dispersions

2.2.2 Preparation of Concrete Enhanced with GNP

After the GNP dispersion was prepared, a drum mixer was used to mix coarse aggregate, sand and cement in dry form for 5 min. The drum mixer was then paused and the specified quantity of GNP dispersion was added. The drum mixer was then restarted and the mixing process continued for an additional 30 min. A schematic illustration of the mixing method is presented in Fig. 3.

2.2.3 Mixture Proportions

The quantities of all materials (cement, sand, coarse aggregates, water, GNP and SP), dispersion techniques and mixing methods used in each mixture are presented in Table 2.

2.3 Testing Methods

The following section summarises the methods used to perform the tests related to fresh properties, mechanical properties and durability of the mixes under investigation.

2.3.1 Determination of Fresh Properties

The slump test was used to assess the workability of each mix and was performed in accordance with AS 1012.3.1 (AS, 1012a). This test was conducted using a slump cone, rod, base plate and ruler. Three layers of fresh concrete mix were poured into the slump cone in accordance with the standard. Each layer of fresh concrete was compacted uniformly using 25 strokes. Finally, the slump of concrete was determined by measuring the difference between the surface height of fresh concrete after cone removal and the slump cone height.

2.3.2 Determination of Mechanical Properties

The compressive strength, flexural strength, and tensile strength were determined in accordance with AS 1012.8 (AS, 1012b), AS 1012.11 (AS, 1012c) and AS 1012.10 (AS, 1012d). For compressive and tensile strength, concrete specimens of nominal diameter of 100 mm and a height of 200 mm were tested. For flexural tensile strength, prismatic specimens of 75 mm × 75 mm × 290 mm were tested in three-point bending. Five concrete specimens were tested for each specific property and the average value was taken.

2.3.3 UPV Test

The UPV is a non-destructive testing method which has been used extensively to assess the homogeneity, uniformity, and quality of concrete. The method can be used to detect internal cracks and other existing defects in concrete structures. Furthermore, it can be used to detect degradation of concrete due to the ingress of liquids or aggressive chemicals. In this study, UPV test was employed to monitor the changes in homogeneity, uniformity and quality of concrete caused by the addition of GNP. The UPV test uses an ultrasonically transmitted pulse to detect the presence of internal voids, cracks and flaws in concrete.

UPV testing was conducted following ASTM C597 (ASTM C597., 2016) standards. The testing setup included a transmitting transducer that emitted a pulse wave into the concrete specimen, and a receiving transducer at the opposite end that detected the pulse. A time measuring unit calculated the travel time of the pulse through the concrete. A schematic illustration of this setup is depicted in Fig. 4a. In this study, a Matest

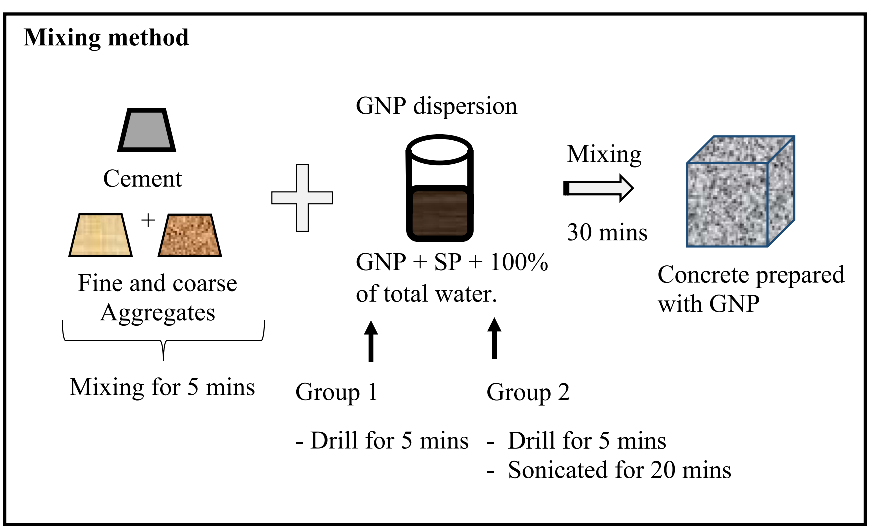

Fig. 3 Schematic representation of mixing procedure used for preparing concrete specimens

Table 2 Summary of mix designations, materials, dispersion techniques, and mixing methods

Mix designation	Cement (kg/m^3)	Fine aggregate (kg/m^3)	7 mm (kg/m^3)	14 mm (kg/m^3)	20 mm (kg/m^3)	Water (kg/m^3)	Dispersion group	Dispersion technique	GNP (wt%)	GNP (kg/m^3)	SP (wt%)	SP (kg/m^3)
D1-A	290	580	369	517	580	174	1	Drill	0.25	0.73	0.0	0.00
D1-B	290	580	369	517	580	174			0.25	0.73	0.2	0.58
D1-C	290	580	369	517	580	174			0.25	0.73	0.4	1.16
D1-D	290	580	369	517	580	174			0.25	0.73	0.6	1.74
D1-E	290	580	369	517	580	174			0.25	0.73	0.8	2.32
D1-F	290	580	369	517	580	174			0.25	0.73	0.9	2.61
D1-G	290	580	369	517	580	174			0.25	0.73	1.0	2.90
D2-A	290	580	369	517	580	174	2	Drill + sonication	0.25	0.73	0.0	0.00
D2-B	290	580	369	517	580	174			0.25	0.73	0.2	0.58
D2-C	290	580	369	517	580	174			0.25	0.73	0.4	1.16
D2-D	290	580	369	517	580	174			0.25	0.73	0.6	1.74
D2-E	290	580	369	517	580	174			0.25	0.73	0.8	2.32
D2-F	290	580	369	517	580	174			0.25	0.73	0.9	2.61
D2-G	290	580	369	517	580	174			0.25	0.73	1.0	2.90

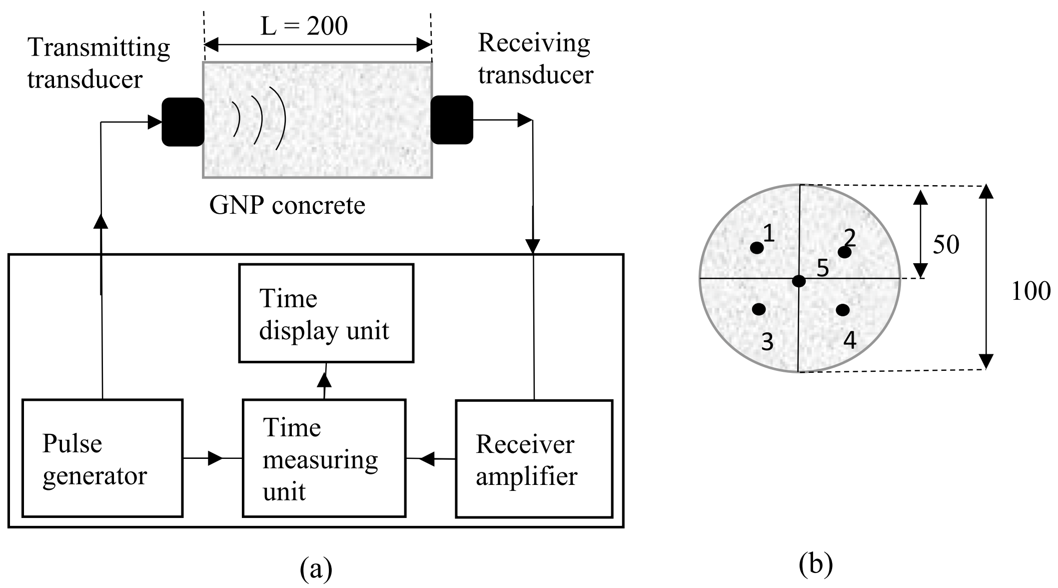

Fig. 4 UVP test, **a** schematic diagram of the test instrument used for UVP and **b** division of the cross-section of each concrete specimen

ultrasonic pulse velocity tester equipped with two 55 kHz probes was used. Five cylindrical concrete specimens, each with a diameter of 100 mm and length of 200 mm, were tested. To ensure accuracy, each specimen's cross section was divided into four zones, as shown in Fig. 4b. Three readings were taken for each zone, with an additional reading in the center of the circular cross section. The average of all five zones' readings represented the UPV value for a single specimen. Results were then averaged across all five specimens to determine the final UPV value.

2.3.4 Water Resistance Analysis

The inclusion of GNP in concrete is expected to improve its mechanical properties. However, enhancing concrete strength alone does not necessarily extend the service life of civil infrastructure, which predominantly depends on concrete durability. Concrete durability is closely tied to its water resistance, influenced by factors, such as pore structure, pore connectivity, and uniformity. In this study, the impact of GNP on concrete water resistance was assessed using the following methods: Ai and AVPV measurements were conducted following AS 1012.21.1999 (AS, 1012e), and initial and secondary sorptivity were determined according to ASTM C1585 (ASTM C, 1585). The procedures for each test are detailed below:

2.3.4.1 A_i and AVPV Concrete specimens with a diameter of 100 mm and a thickness of 50 mm were used to calculate the A_i and AVPV. For each measurement, five specimens were examined and the average value was calculated. To determine A_i, concrete specimens were dried in an oven at 100 ± 2 °C for 24 h until a constant mass was reached. Afterward, the concrete specimens were removed from the oven and allowed to cool to a temperature of 23 ± 2 °C and weighed. The mass of the oven-dry concrete specimens was identified as M_d. After measuring M_d, concrete specimens were immersed in water at a temperature of approximately 21 °C for 48 h. Concrete specimens were removed from the bath water and the surface moisture was dried with a towel. The mass of the surface-dry and saturated concrete specimens was identified as M_s. Equation (1) was used to calculate A_i:

$$A_i = \left(\frac{M_s - M_d}{M_d} \right) \times 100\% \tag{1}$$

where:

$$M_s = \text{mass of surface} - \text{dry and saturated specimens(g)}$$

$$M_d = \text{oven} - \text{dry mass of specimens(g)}$$

To measure AVPV, the surface-dry specimens were immersed in a water bath and boiled for 5.5 h. After cooling in the water bath to approximately 23 ± 2 °C, each specimen was removed and surface moisture was dried with a towel. The mass of the boiled specimens M_{boiled} was recorded. Subsequently, the weight of the specimens suspended in water $M_{suspend}$ was determined. AVPV was then calculated using the following equation:

$$AVPV = \left(\frac{M_{boiled} - M_d}{M_{boiled} - M_{suspend}}\right) * 100\% \quad (2)$$

where:

M_{boiled} = mass of specimens after boiling (g).
M_d = oven-dry mass of specimens (g).
$M_{suspend}$ = mass of suspended specimens (g).

2.3.4.2 Initial and Secondary Sorptivity The rate of absorption (sorptivity) of water of concrete specimens was determined according to ASTM C 1585 (ASTM C, 1585). This method involves measuring the increase in mass of a concrete specimen over time, with only one surface exposed to water. A schematic illustration of the test setup is provided in Fig. 5. Concrete specimens, having a nominal diameter of 100 mm and a thickness of 50 mm, were utilized. These specimens were initially placed in an environmental chamber at 50 ± 2 °C and 80 ± 3% relative humidity (RH) for 3 days. Subsequently, each specimen was transferred to a separate sealable container maintained at 23 ± 2 °C for 15 days before commencing the absorption procedure. Specimens were removed from the sealable container, where they were sealed with epoxy on their circular surface to avoid the ingress of water. The part of the specimens that was not exposed to water, was sealed with a plastic sheet. The mass of the sealed specimens was measured and identified as the initial mass of water absorption for the calculation. The sealed specimens were placed at the bottom of a container, then the container was filled with water. The level of the water was maintained at 1 to 3 mm above the top of stainless-steel rods. For the calculation of initial sorptivity of specimens, the mass of specimens was recorded after 1, 5, 10, 20, 30, 60, 120, 180, 240, 300, and 360 min. For the calculation of the secondary sorptivity of specimens, the mass of the specimens was recorded once per day for 9 days.

Equation (3) was used to calculate the initial and secondary water absorption rate:

$$\mathrm{I} = \frac{M_t}{a/b} \quad (3)$$

where:

I = absorption

M_t = the variation of the mass of the concrete specimens at the time t (g)

a = the area of the concrete specimens that is exposed to water (mm^2)

b = the density of the water (g/mm^3)

The initial and secondary rate of water absorption was determined as the slope of the line that is the best fit to the absorption (I) plotted against the square root of time. The slope is calculated by least-square linear regression analysis of the plot of absorption (I) versus the square root of time.

2.3.5 Microstructure Analysis

Modification of the microstructure of concrete may result in an improvement of its macro properties. To investigate the effect of GNP on the microstructure of concrete specimens, GNP modified concrete samples were examined using SEM micrographs and EDS elemental maps at 28 days. The SEM micrographs were used to study the morphology of concrete samples. SEM and EDS observation is performed on the broken surface of concrete samples. These samples were collected from concrete specimens after performing compressive strength test at

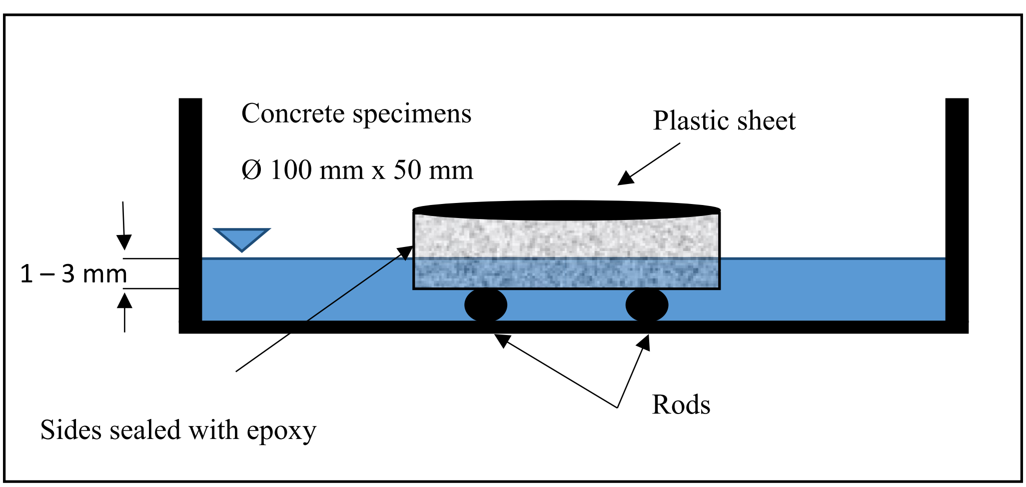

Fig. 5 Schematic representation of setup test for initial and secondary sorptivity

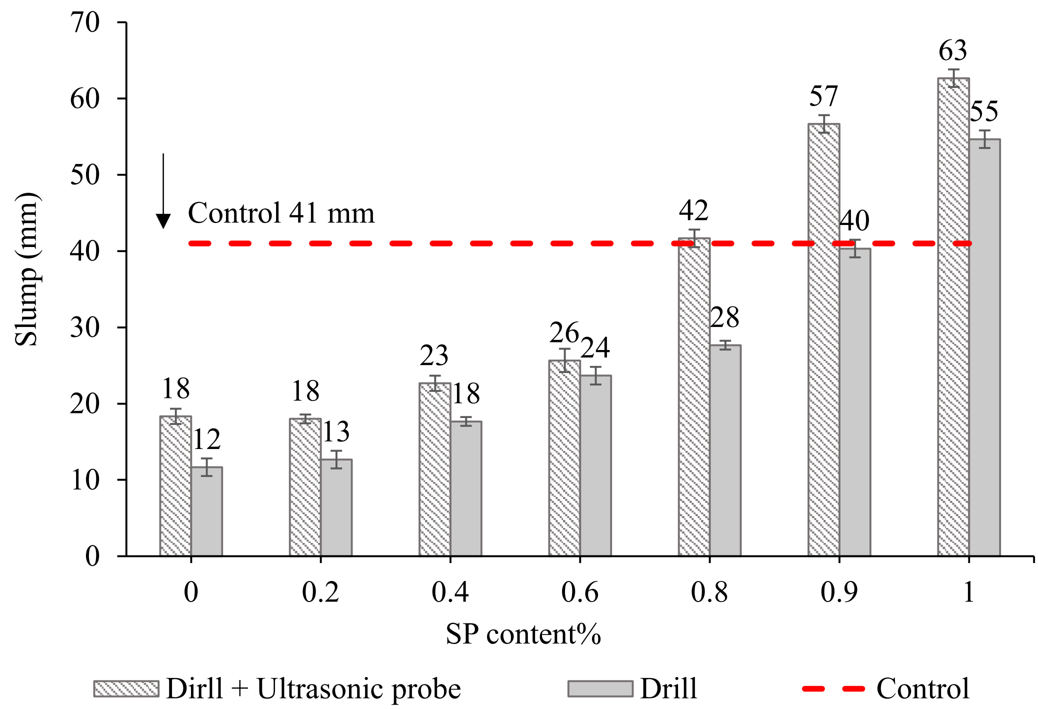

Fig. 6 Results for slump test of control mix and mixes prepared with non-sonicated and sonicated GNP dispersions

28 days. EDS was used to verify the presence of GNP in the sample. In this study, a ZEISS Supra 40 VP scanning electron microscope was used.

3 Results and Discussion

3.1 Fresh Properties

The slump results for fresh concrete mixes are plotted in Fig. 6 which provides insights into the effect of GNP additives on the workability of concrete. In general, it was found that the addition of 0.25 wt% GNP reduced the slump values of all fresh concrete mixes irrespective of the mixing method. More specifically, the slump value of fresh mixes prepared with non-sonicated GNP dispersion (D1-A) reduced from 41 to 12 mm, while the slump value of fresh mixes prepared with sonicated GNP dispersion (D2-A) decreased from 41 to 18 mm. This represented a reduction in workability of 72% and 55% with respect to the control mix. This reduction in workability can be attributed to the attachment of water molecules to the surface of GNP which cause a reduction in the available water required for workability (Simpkins et al., 1989). As water molecules adhere to the surface or between adjacent layers of GNP, they form hydrogen bonds on the surface or between adjacent layers. The hydrogen bonds are retained on the surface or within the adjacent layers, forming statistically stable structures over time (Akaishi et al., 2017). Similar results were observed by Wang et al. (Wang et al., 2016) and Chen et al. (Chen et al., 2019) who also reported that the addition of GNP reduced the workability of fresh concrete and fresh paste mixes, respectively.

In the construction industry, the slump value is used to evaluate the quality and suitability of a concrete mix for a specific application. The slump value of concrete is important to ensure that concrete can be easily pumped, placed, compacted and finished. As a result, the reduction in slump values observed by the addition of GNP to concrete must be minimised. Research has suggested that a number of surfactants, including SP (Papanikolaou et al., 2021b), nonylphenylethers (Igepal, CO890) (Wang & Shuang, 2018; Wang & Zhao, 2017), sodium dodecyl benzene sulfonate (SDBS) (Shuang et al., 2022) and solvents, such as methylcellulose (MC) (Tong et al., 2016), have been used to mitigate the negative effects of GNP on workability of cement composites. SP such as polycarboxylate, lignosulphonate and naphthalene-based are widely used in the construction industry. Since polycarboxylate-based SP (polycarboxylate ether and modified polycarboxylic ether) have been demonstrated to be more efficient at dispersing GNP compared to lignosulphonate and naphthalene-based SP (Papanikolaou et al., 2021b), a polycarboxylate-based SP was selected as a dispersant agent to mitigate the negative effect of GNP on the slump values of fresh concrete mixes in the present study. Figure 6 summarises the slump for concrete mixes with 0.25 wt% GNP when SP concentrations between 0 and 1% were added. While the mix containing no GNP had a slump value of 41 mm, this was reduced to 18 mm when adding 0.25 wt% GNP with sonication. However, adding SP of 0.8 wt% was shown to improve the slump from 18 to 42 mm which was comparable to the control mix when sonication was used. If only drill mixing is used, then the optimal SP content should be increased to 0.9 wt% to achieve a slump of 40 mm. This increase may be due to the fact that the drill generates less energy than an ultrasonic probe which is less effective to de-agglomerate the GNP in water (Xu et al., 2018). The agglomeration of GNP obstructs the physical interaction between water and cement grains, reducing their chemical reaction (Du & Pang, 2018), thus negative affecting the workability of concrete.

3.2 Mechanical Properties

After determining the optimal SP content to mitigate the negative effects of GNP on concrete slump and workability, an evaluation of the strength of concrete specimens prepared with non-sonicated and sonicated GNP dispersions containing the optimal SP content was assessed.

3.2.1 Compressive Strength

The results of compressive strength of control specimens, D1-F and D2-E at 7, 14 and 28 days are plotted in Fig. 7. Examining the results, it can be observed that the cylindrical compressive strength (f_{cu}) of the control specimens was 22.5 MPa, 26.7 MPa, and 31.7 MPa, at 7, 14, and 28 days, respectively. In comparison, the compressive strength of sonicated mix D2-E containing 0.25 wt% GNP and 0.8% SP was 26.8 MPa, 31.9 MPa, and 38.3 MPa at 7, 14, and 28 days, respectively, which represented an improvement of 19.0%, 19.4%, and 20.8% compared to control specimens. Compressive strength was thought to be improved due to GNP reinforcing the microstructure of the cement matrix (Chen et al., 2018; Shuang et al., 2022; Wang et al., 2016). Moreover, compressive strength of D1-F which did not utilise sonication was 25.1 MPa, 29.9 MPa and 35.9 MPa at 7, 14, and 28 days, indicating an enhancement of 11.4%, 11.7%, and 13.2% with respect to control specimens. This result indicated that the addition of non-sonicated GNP dispersion had a lower impact on compressive strength. Other researchers also used the combination of sonication treatment and SP to achieve the best performance on compressive strength of cement composites (Dalla et al., 2021; Liu et al., 2016; Wang & Pang, 2019). In contrast, Du et al. (Du et al., 2016) prepared concrete specimens with GNP ranging from 0.5 to 2.5 wt% and reported that the addition of GNP resulted in a negligible effect on mechanical properties. This null effect on mechanical properties may be due to the high amount of GNP added to concrete as most studies have shown that the optimal content of GNP is less than 0.5 wt%. The addition of high amount of GNP has been shown to result in agglomeration reducing the uniform distribution of nanosheets in the cement system resulting in decreasing the nucleation sites, thus having a null impact on macro-properties of concrete.

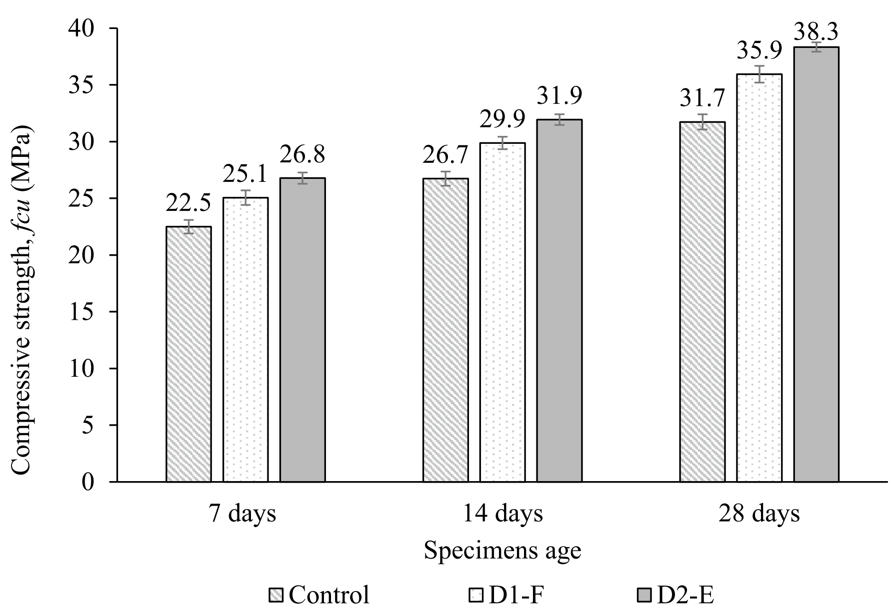

Fig. 7 Summary of compressive strength results for control, non-sonicated (D1-F) and sonicated specimens (D2-E)

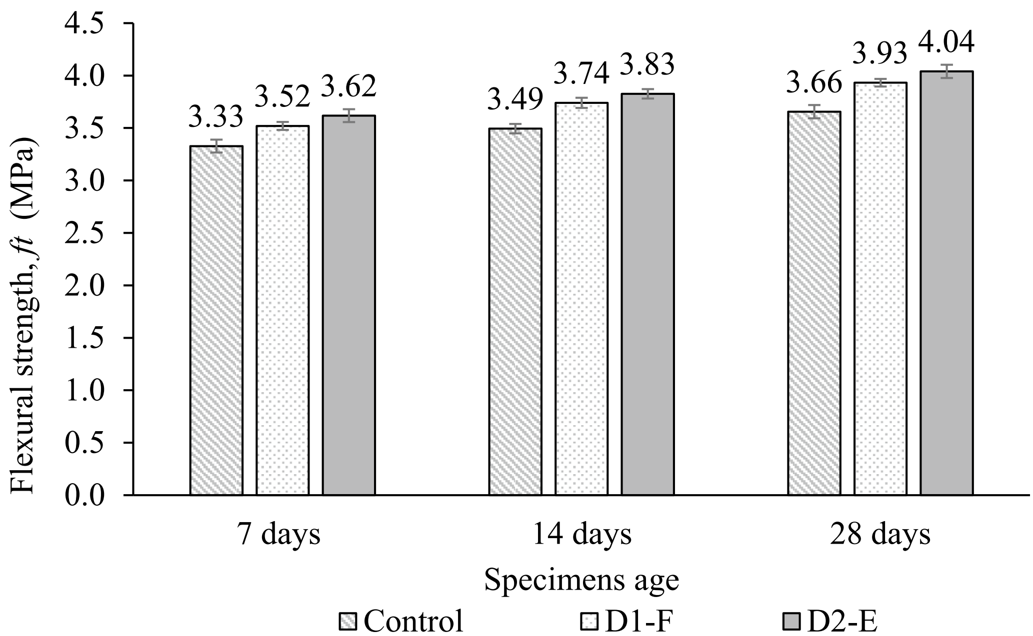

Fig. 8 Summary of flexural tensile strength results for control, non-sonicated (D1-F) and sonicated specimens (D2-E)

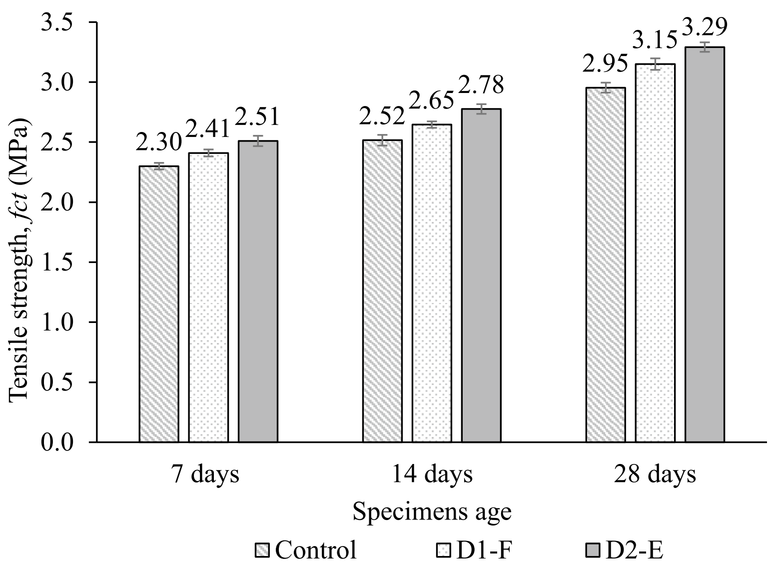

Fig. 9 Summary of splitting tensile strength results for control, non-sonicated (D1-F) and sonicated specimens (D2-E)

3.2.2 Flexural and Tensile Strength

The results of flexural and tensile strength of control specimens, D1-F, D2-E at 7, 14 and 28 days are plotted in Figs. 8 and 9. The maximum improvement in flexural and tensile strength was observed in specimen D2-E, where the flexural strength was increased by 8.7%, 9.5%, and 10.5% at 7, 14, and 28 days, compared to control specimens. Furthermore, splitting tensile strength of D2-E was enhanced by 9.1%, 10.3%, and 11.4%, at 7, 14 and 28 days when compared to control specimens. Other studies have also reported an improvement in flexural strength of GNP reinforced cement composites. For instance, Wang et al. (Wang et al., 2016) found that the addition of 0.05 wt% GNP increased flexural strength of cement paste by 23.7% and 16.8% at 7 and 28 days. In their study, the stability of GNP dispersion was improved using methylcellulose (MC) which is commonly used as a water-retaining agent and retarder of cement paste or mortar in the construction industry. Jiang et al. reported that the addition of 0.075 wt% GNP increased flexural strength by 5.8% (Jiang et al., 2021). In their study, the GNP dispersion was prepared without sonication treatment which may explain the lower improvement compared to our results. It can also be observed from Figs. 8 and 9 that D1-F showed a lower improvement in flexural and tensile strength compared to D2-E which indicated that the addition of non-sonicated GNP dispersion prepared with SP was less effective in terms of improving both properties. These results can be explained by the fact that the nanosheets in the non-sonicated GNP dispersion are less stable and more agglomerated (Sandhya et al., 2021) which result in lower strengthening of the cement matrix.

3.3 Homogeneity and Water Resistance

The structural integrity of concrete civil infrastructure is linked to the durability and quality of material which highly depends on its resistance to the ingress of fluids (primarily water) and gases, such as carbon dioxide (Bentz et al., 1999; Gjørv, 2011; Han et al., 2013). This section summarises the results of an investigation into the influence of GNP on the quality and homogeneity of concrete specimens which was evaluated using UPV testing. Next, the effect of GNP on concrete water resistance was examined by measuring Ai, AVPV and sorptivity (initial and secondary sorptivity).

3.3.1 UPV Assessment

In this subsection, we discuss the effect of GNP on concrete homogeneity and uniformity using UPV testing. The higher the homogeneity and uniformity of concrete, the better the quality of concrete. Based on the UPV range (km/s), concrete quality can be classified as excellent (>4.5 km/s), good (3.5–4.5 km/s), questionable (3.0–3.5 km/s), poor (2.0–3.0 km/s) and very poor (less 2.0) (Whitehurst xxxx). The results of UPV test of unmodified control samples, D1-F and D2-E are plotted in Fig. 10. Overall, it was observed that the concrete mixes prepared with GNP had higher UPV values, which may be attributed to the fact that GNP refined the pore structure of cement matrix, resulting in a more homogeneous and uniform microstructure, thus increasing the quality of concrete. Furthermore, the UPV values of control concrete, D1-F and D2-E at 28 days were 4.07 km/s, 4.42 km/s and 4.60 km/s, respectively. UPV values of control specimens and D1-F range between 3.5 km/s and 4.5 km/s, which indicates that the quality of those concrete specimens was good. The UPV value of D2-E was higher than 4.5 km/s, indicating the quality of concrete specimens was excellent. It was noted that the highest increase in pulse velocity was observed in concrete specimens containing GNP dispersion prepared with sonication treatment and SP. Indeed, UPV values of D2-E increased by 11.7%, 12.5% and 12.9% at 7, 14 and 28 days, respectively, with respect to control. By contrast, the UPV values of D1-F increased by 8.0%, 8.4% and 8.6% at 7, 14,

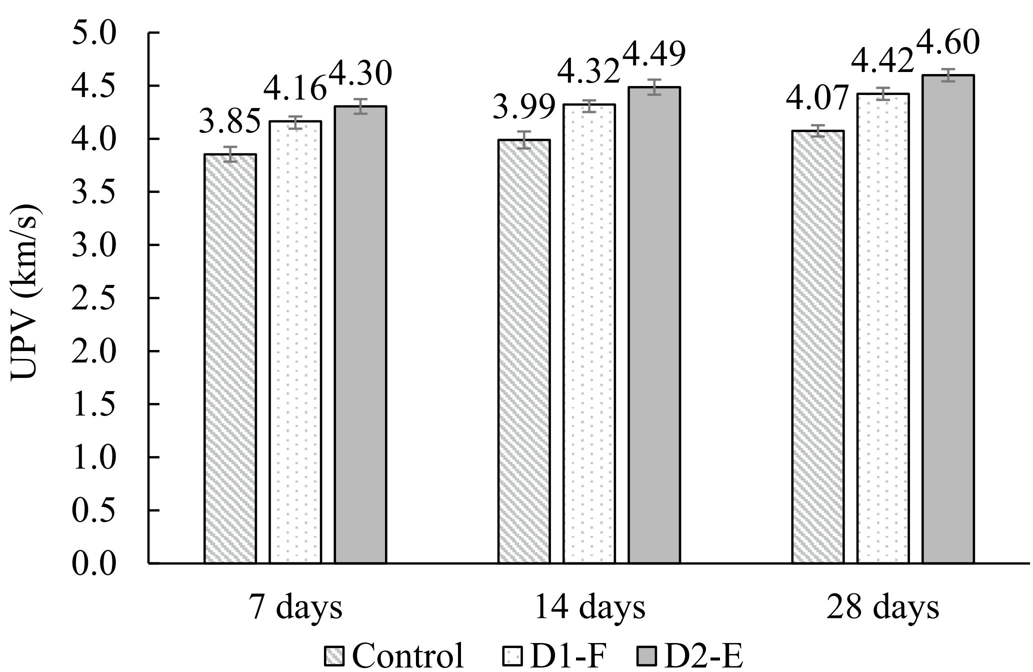

Fig. 10 Results for UPV test for control specimens, D1-F and D2-E

and 28 days. The results support those found previously in Sect. Mechanical properties, where the addition of sonicated GNP dispersion (D2-E) (SP: 0.8 wt%) resulted in a higher increase in strength of concrete specimens. Previous studies also reported that the addition of GNP increased the UPV values of cement composites (Ahmad et al., 2022; Arslan et al., 2022). For instance, Ahmad et al. (Ahmad et al., 2022) found that the UPV values of concrete specimens increased from 3.8 km/s to 4.2 km/s when 5 wt% GNP was added. Furthermore, Arslan et al. (Arslan et al., 2022) reported that the addition of 0.14 wt% GNP to mortar specimens increased the UPV values from 4.6 km/s to 4.9 km/s. Arslan et al.(Arslan et al., 2022) and Ahmad et al. (Ahmad et al., 2022) claimed that GNP reduced the porosity of cement composites at the nanoscale, thus improving the homogeneity and quality of concrete.

3.3.2 A_i and AVPV Assessment

The results of A_i and AVPV are plotted in Figs. 11 and 12 which showed that A_i and AVPV were reduced by adding GNP at all ages. For instance, after 28 days, D1-F and D2-E experienced 19.4% and 28.3%, lower A_i rate when compared to control specimens. While for the same curing period, the AVPV values of D1-F and D2-E were reduced by 19.9% and 26.3%, respectively. This reduction is attributed to the fact GNP may also refine the pore structure of cement matrix by the nucleation and filling effects (Du et al., 2016). This increased the uniformity of the microstructure of the cement matrix and reduced the voids and pore interconnectivity in the concrete (Tong et al., 2016), preventing water from entering the concrete specimens. Similar observations were made by Akono (Akono, 2021) who reported that adding 0.5 wt%

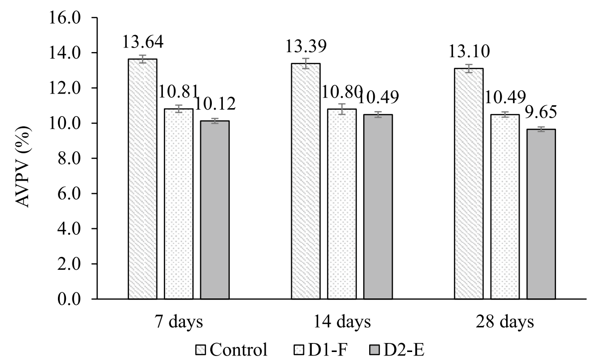

Fig. 12 Results for AVPV test for control specimens, D1-F and D2-E at 7, 14 and 28 days

GNP reduced the water absorption in cement paste and claimed that this reduction was due to the reduction of amount of pores and the compaction of the microstructure of the specimens. Furthermore, it is important to highlight that in the present study, the highest reduction in A_i and AVPV were observed when concrete specimens were cast with sonicated GNP dispersion prepared with SP. These results may be due to the agglomeration of nanosheets in non-sonicated GNP dispersion diminishing the positive effects from filling pores and reducing nucleation sites for hydration products, which in turn reduced the beneficial effects of GNP on the water resistance of concrete. These results are in good agreement with those found in Sect. UPV assessment, where concrete specimens prepared with the sonicated GNP dispersion had the highest increase in UPV values. Furthermore, according to VicRoads technical note 89 (Technical & note 89, Test methods for the assessment of durability of concrete, 2007), OPC concrete with AVPV

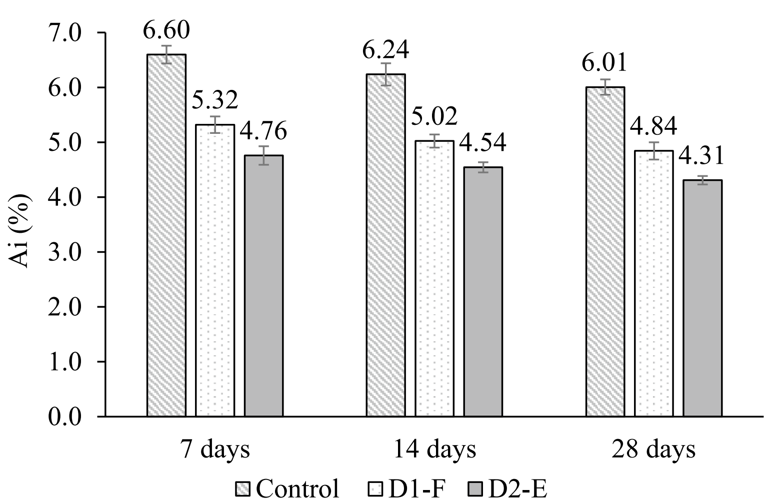

Fig. 11 Results for A_i test for control specimens, D1-F and D2-E at 7, 14 and 28 days

values less than 13% is classified as good-quality concrete which possesses low pore interconnectivity. Based on these results, it can be also highlighted that concrete specimens prepared with GNP had AVPV values below 13%. Therefore, D1-F and D2-E can be classified as good quality concrete with limited pore interconnectivity.

3.3.3 Sorptivity Assessment

Another widely accepted method to assess the water resistance of concrete is the uniaxial water absorption test or water sorptivity test. The water sorptivity of concrete is defined as the rate at which water is absorbed by capillary and gel pores. Moreover, the rate of water sorptivity is highly influenced by the total porosity and pore structure of concrete (Bentz et al., 1999; Hanzic & Ilic, 2003). Water sorptivity in concrete is divided into two main phases: initial and secondary sorptivity. First, in terms of the initial sorptivity, the initial rate of water absorption begins immediately after concrete is immersed in water and lasts for up to 6 h. A

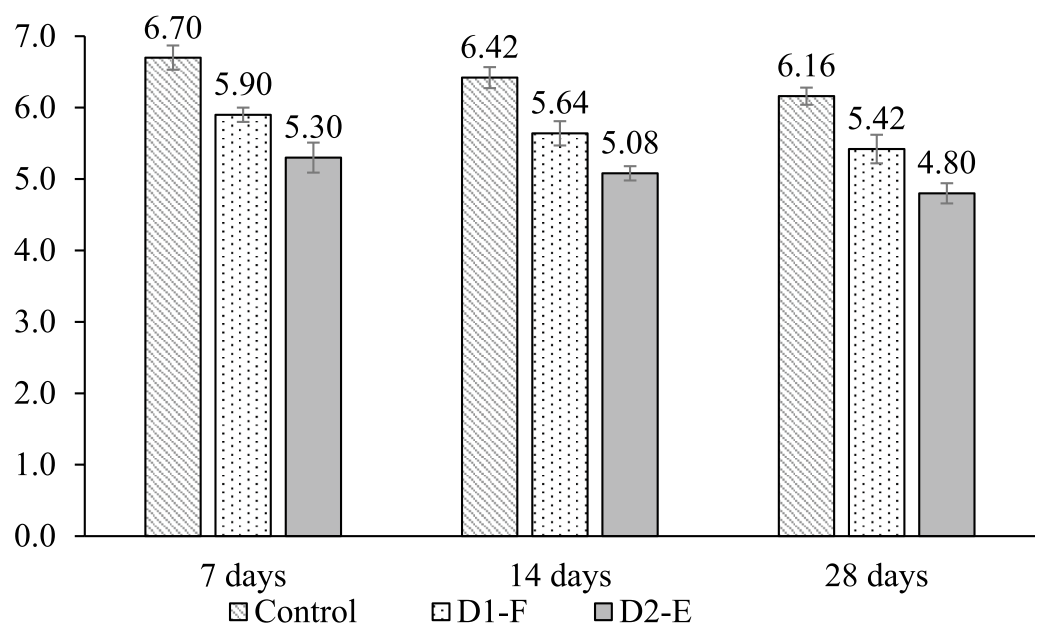

Fig. 13 Results for initial sorptivity for control specimens, D1-F and D2-E at 7, 14 and 28 days

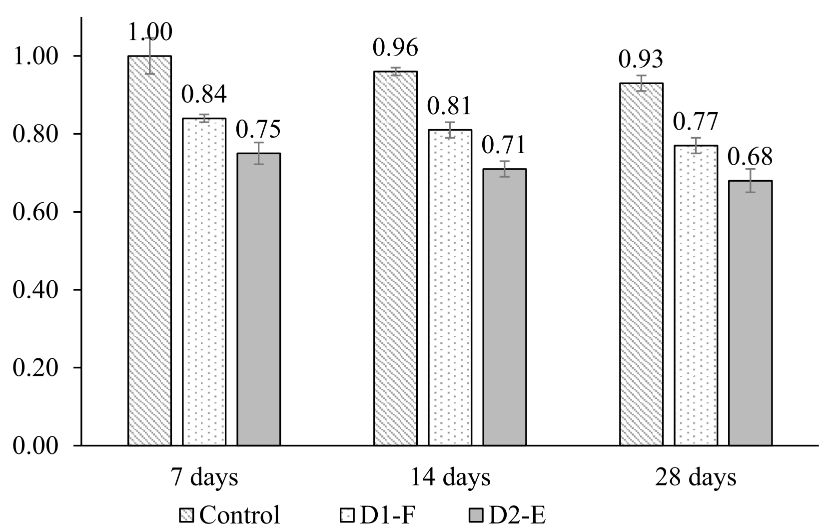

Fig. 14 Results for secondary sorptivity for control specimens, D1-F and D2-E at 7, 14 and 28 days

measurement of the initial rate of water absorption is influenced by the amount of capillary pores. Second, regarding secondary sorptivity, the secondary rate of water absorption of concrete occurs between 6 h and 7 days. Measurements of secondary rate of water absorption are affected by the size of the gel pores (Arslan et al., 2022; Safuta et al., 2021). In cement composites, capillary pores have a pore size of up to 10 µm, while gel pores have a pores size less than 10 nm (Dong et al., 2017). The results of the initial and secondary rates of water absorption of control and specimens D1-F and D2-E at 7, 14 and 28 days are plotted in Figs. 13 and 14, respectively. From the results, it can be observed that the addition of GNP decreased both the initial and secondary rate of water absorption of concrete specimens at all ages. The initial rate of water absorption of D2-E at 28 days was decreased by 22% (from 6.16×10^{-3} mm/sec$^{0.5}$ to 4.80 x 10^{-3} mm/sec$^{0.5}$), while the secondary rate of water absorption was decreased by 27% (from 0.93 10^{-3} mm/sec$^{0.5}$ to 0.68 mm/sec$^{0.5}$). These results indicated that the addition of GNP modified the pore structure of the concrete specimens. This refinement in the pore structure of concrete is due to the nucleation and filling effect of GNP, which promoted a denser microstructure (Wu et al., 2021). A similar conclusion was reported by Arslan et al. (Arslan et al., 2022) who reported that the addition of 0.14 wt% GNP decreased initial and secondary water absorption of mortar specimens by 30.6% and 34.8%, respectively, compared to control specimens. They claimed that this reduction was due to the fact that GNP reinforced the interfacial transition zone (ITZ) and filled the capillary voids in cement matrix, thus reducing the rate of water sorptivity. Safuta et al. (Safuta et al., 2021) reported that the addition of 0.05 wt% graphene reduced the initial and secondary sorptivity of mortar specimens at 28 days by 21% and 25%, respectively. The reduction in sorptivity was attributed to the refinement of capillary pores and C–S–H gel formation. Furthermore, in the present study, it was also noticed that the reduction of initial and secondary rates of absorption were less noticeable in D1-F. These results are consistent with the results of UPV in Sec. UPV assessment and A_i and AVPV in Sect. A_{i} and AVPV Assessment which showed that sonicated GNP dispersion containing SP was most beneficial for refining pore structure of concrete.

3.4 Microstructure Analysis

Improving the macro properties of cement composites can be achieved by modifying its microstructure (Souza et al., 2022; Wu et al., 2021). Therefore, to examine the effects of GNP on the microstructure of concrete specimens, SEM observations were conducted. The results are presented in two sections, the first relates to the SEM observation of plain concrete, followed by microscopic analysis of concrete prepared with GNP. The second part of the discussion proposes a mechanism for the reinforcement of concrete microstructure.

3.4.1 Microscopic Observations of Plain Concrete

First, small pieces of plain concrete specimens were analysed using an SEM test. In the SEM photographs, the presence of various cement hydration products can be observed. These cement hydration products are formed when cement grains and water react chemically (Taylor, 1997). Calcium–silica–hydrate (C–S–H) gels contribute the most to the strength of concrete and can be observed in Fig. 15a, b. C–S–H gels normally appear in the form of foils or needle-oriented foils (Richardson, 1999). Calcium hydroxide (C–H), which has hexagonal plate structures is another important component generated during cement hydration process (Gallucci & Scrivener, 2007) can be observed in Fig. 15a, b. It can be seen that ettringite another constituent of cement hydration process was formed in the wall of air voids. Ettringite is typically found in large quantities as rod-like crystals in the early stages of cement hydration and can be also formed in minor amounts within air voids or pores of mature concrete (Taylor, 1997). In addition, pores, voids and microcracks can be also observed in the images.

3.4.2 Microscopic Observations of Concrete Prepared with GNP

To investigate the physical interaction between GNP and cement hydration products, mix D2-E which showed higher performance was selected. For the microstructure analysis, small pieces of D2-E were examined using SEM micrographs and EDS elemental maps. First, the morphology of D2-E was observed using SEM micrographs. Second, to confirm the presence of GNP, the EDS elemental map in a specific zone of sample was captured to detect carbon element. From the images, various components of the cement matrix can be observed. Cement hydration products such as C–S–H gel and C–H have the same morphology as plain concrete samples. This suggested that GNP did not modify the morphology of those cement hydration products. This observation was confirmed by previous researchers who reported that GNP do not alter the morphology and microstructure of cement hydration products (Akono, 2021; Wang & Pang, 2019). Furthermore, the EDS mapping of the SEM micrograph is displayed in Fig. 16 and revealed a very high detection of carbon element, confirming the presence of GNP. After confirming the presence of carbon element, to analyse the morphology of the sample in this zone in more detail, additional SEM micrographs were captured. From examining Fig. 17a, it can be observed that C–S–H

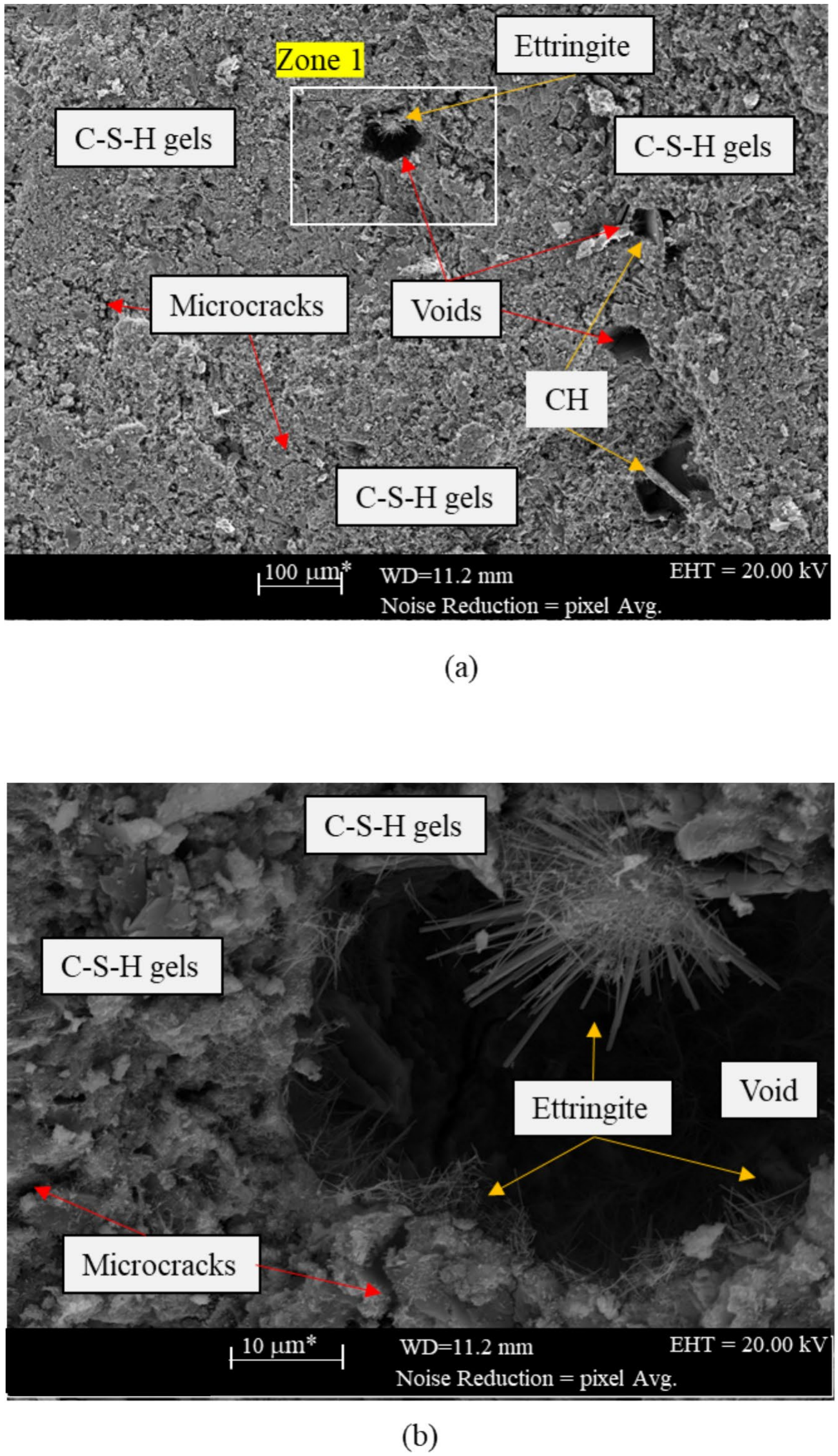

Fig. 15 SEM images of plain concrete specimens at 28 days (**a**) total zone analyzed and (**b**) zoom of zone 1

products were formed at the interface with GNP. C–S–H products may precipitate on the interface with the GNP, and then started to grow in different in plate directions, covering various areas of the surface of the GNP. It can also be observed that C–S–H products were distributed at different locations on the surface of GNP, which

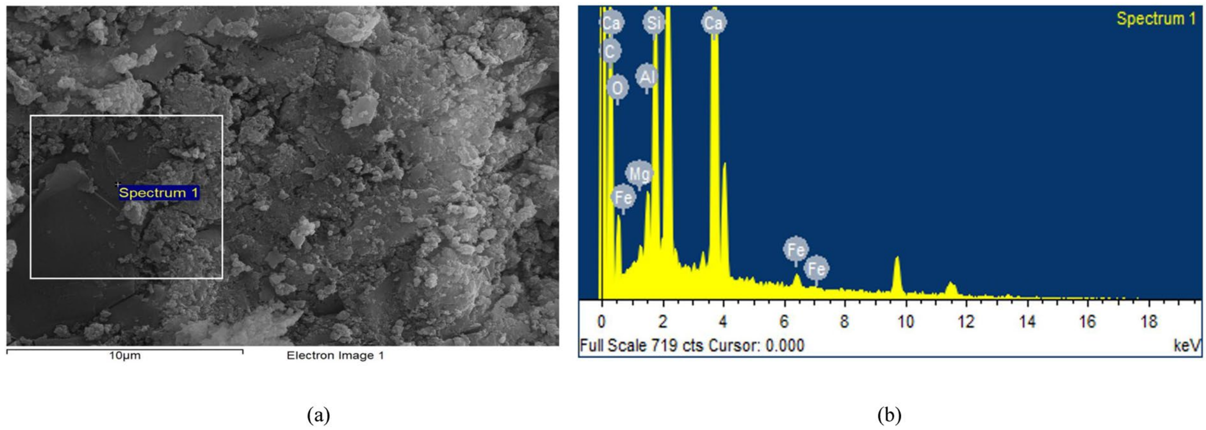

Fig. 16 EDS elemental test (***a***) the zone where the EDS analysis was conducted, (***b***) results of the EDS analysis

created strong interface bonding between the GNP and the cement matrix. This strong interface bonding can transfer stresses effectively, controlling the propagation of cracks under external load (Wang et al., 2016). In the next step, to further analyse the physical interaction between GNP and cement hydration products, two zones, zone

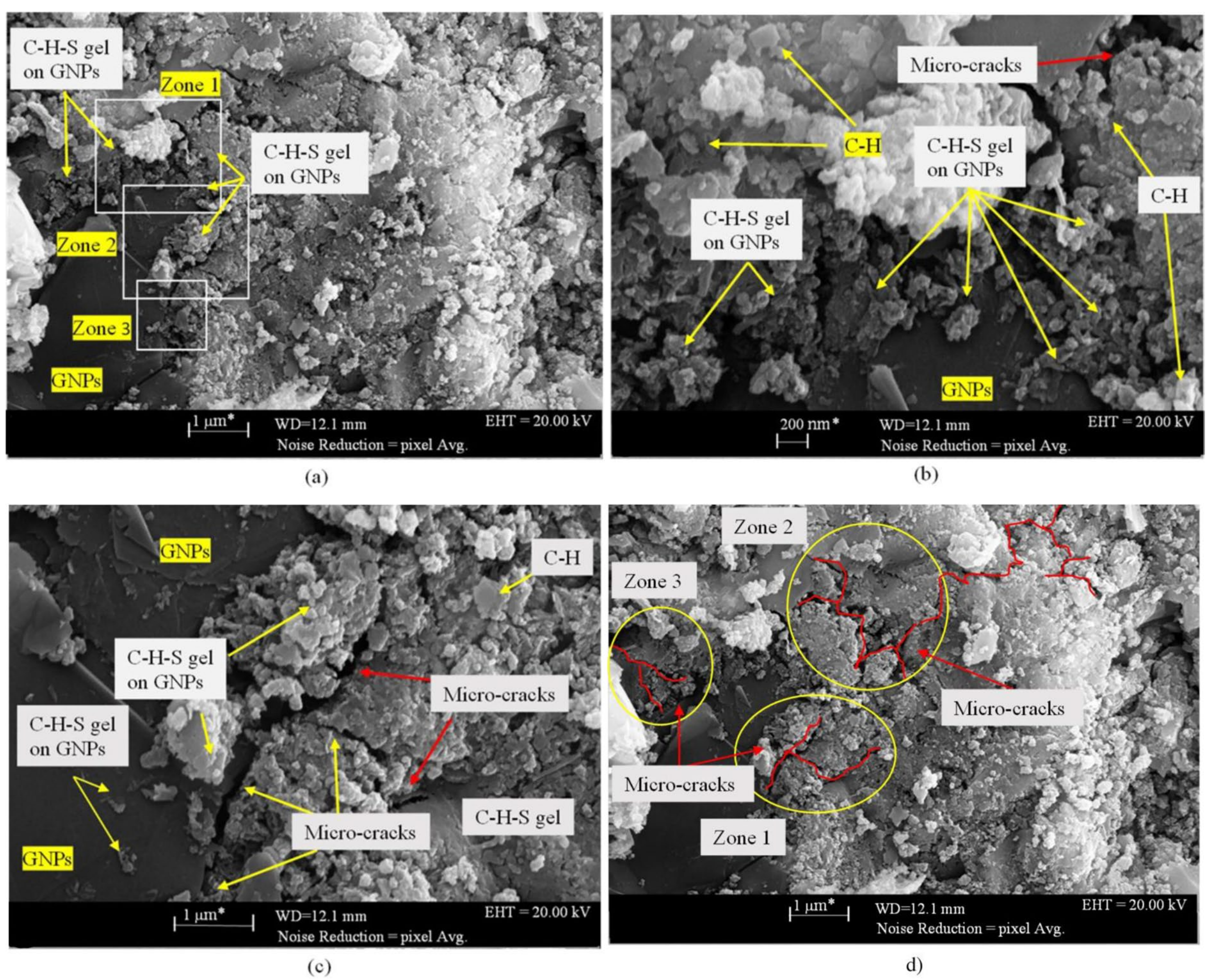

Fig. 17 SEM micrographs of sample, (**a**) total zone analysed, (**b**) zoom of the zone 1, (**c**) zoom of the zone 2, (**d**) crack pattern surrounding GNP

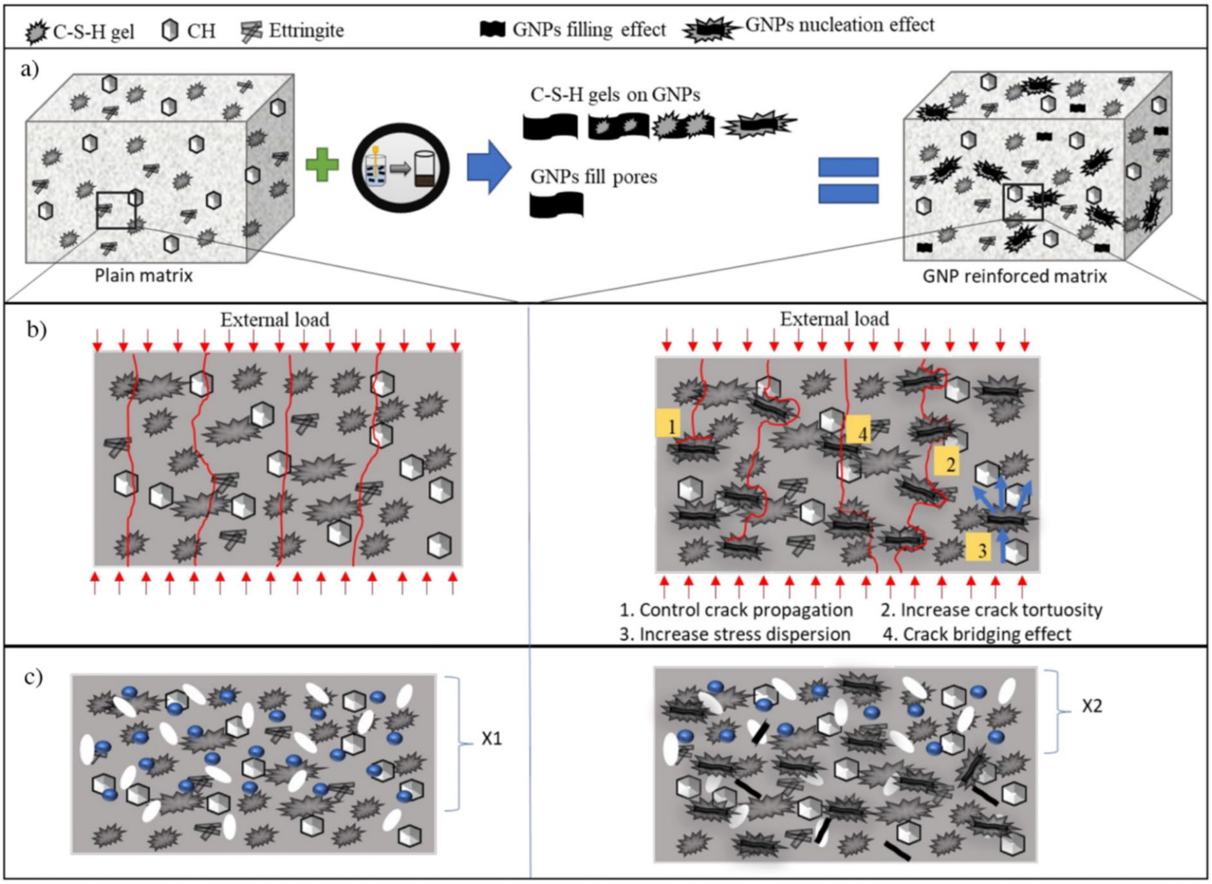

Fig. 18 Schematic representation of the mechanism for the nano reinforming of concrete prepared with GNP; (**a**) precipitation of C–S–H gel on GNP; (**b**) illustrates the strengthening of the nanostructure which contributes to enhancing the strength of concrete; (**c**) illustrates the refinement of pore structure which benefits water resistance of concrete (X1: water penetration level for plain concrete, X2: water penetration level for concrete prepared with GNP)

A-1 and zone A-2 were selected. Figure 17b, c depicts with greater clarity the precipitation of cement hydration products, particularly C–S–H gels on the surface of the GNP. This indicated that GNP serve as nucleation sites for the growth of hydration products, especially C–S–H gels. The hydration products deposited on the surface of the GNP formed a strong structure, which can be considered a more compact and homogeneous microstructure (Adhikary et al., 2022; Akono, 2021). A further analysis was conducted to examine the development of cracks surrounding GNP. Figure 17d displays the microcrack pattern around GNP. Microcracks were formed in zones D-1, D-2 and D-3, as shown in Fig. 17d. In zone D-1, it was observed that the nucleation effect of GNP can lead to crack branching, where a single microcrack bifurcates. The increase in the crack branching extends the path of cracks, preventing premature fracture of concrete. In zones D-2 and D-3, it can be seen that the propagation of the microcracks was controlled by GNP and the C–S–H gels precipitated on their surface, which would contribute to enhance the strength of concrete. Similar studies also reported that GNP control crack propagation by densifying the microstructure of cement matrix and promoting the development of crack branching (Baomin & Shuang, 2019; Wang & Pang, 2019). In addition, GNP have a bridging effect which helps to distribute stress throughout the material (Baomin & Shuang, 2019; Lin & Du, 2020). Another benefit of the refinement of the microstructure of cement matrix by GNP is the increase in crack tortuosity (Du & Pang, 2015). Furthermore, the nucleation effect of GNP refines the pore structure of the cement matrix, resulting in a more homogeneous and uniform material (Lin & Du, 2020). Moreover, GNP can also fill the pores of the microstructure of sample (Adhikary et al., 2022; Akono, 2021; Du & Pang, 2015).

3.4.3 Proposed Reinforcing Mechanism

Based on experimental evidence presented in this study and previous research data from the literature, we propose a mechanism for the nano reinforming of concrete prepared with GNP, to enhance its strength and durability:

1. Using appropriate sonication methods for dispersion, there should be random arrangements of GNP within the cement matrix during the hydration process.
2. During the hydration process, GNP serve as 2D platforms, where cement hydration products, particularly C–S–H gels are precipitated and grown. As cement hydration products grow on the surface of the GNP, denser clusters of structures are formed covering different areas of the GNP. These nucleation effects occur in different parts of the cement matrix. A schematic representation of nucleation effect is presented in Fig. 18a.
3. The formation of dense clusters of C–S–H gels on the surface of the GNP provides a strong bond and efficient interlinking between the nanoparticles and the rest of the cement hydration products, thus strengthening the cement matrix.
4. The strengthening of the nanostructure of the cement matrix using GNP benefits the stress distribution throughout the material during loading. In addition, the enhanced microstructure also increases cracking tortuosity and prevents crack propagation in concrete. Therefore, the macro-performance of concrete is improved in terms of strength. A schematic representation of the strengthening of cement matrix is illustrated in Fig. 18c.
5. The nucleation effect of GNP refines the pore structure of the cement matrix, resulting in a more homogeneous and uniform material. This refinement of microstructure controls the ingress of liquid into concrete and creates a more tortuous path for water to enter and move through concrete. This results in enhancing the water resistance of the material, thus improving the durability performance of concrete. A schematic representation of the refinement of pore structure is showed in Fig. 18b.

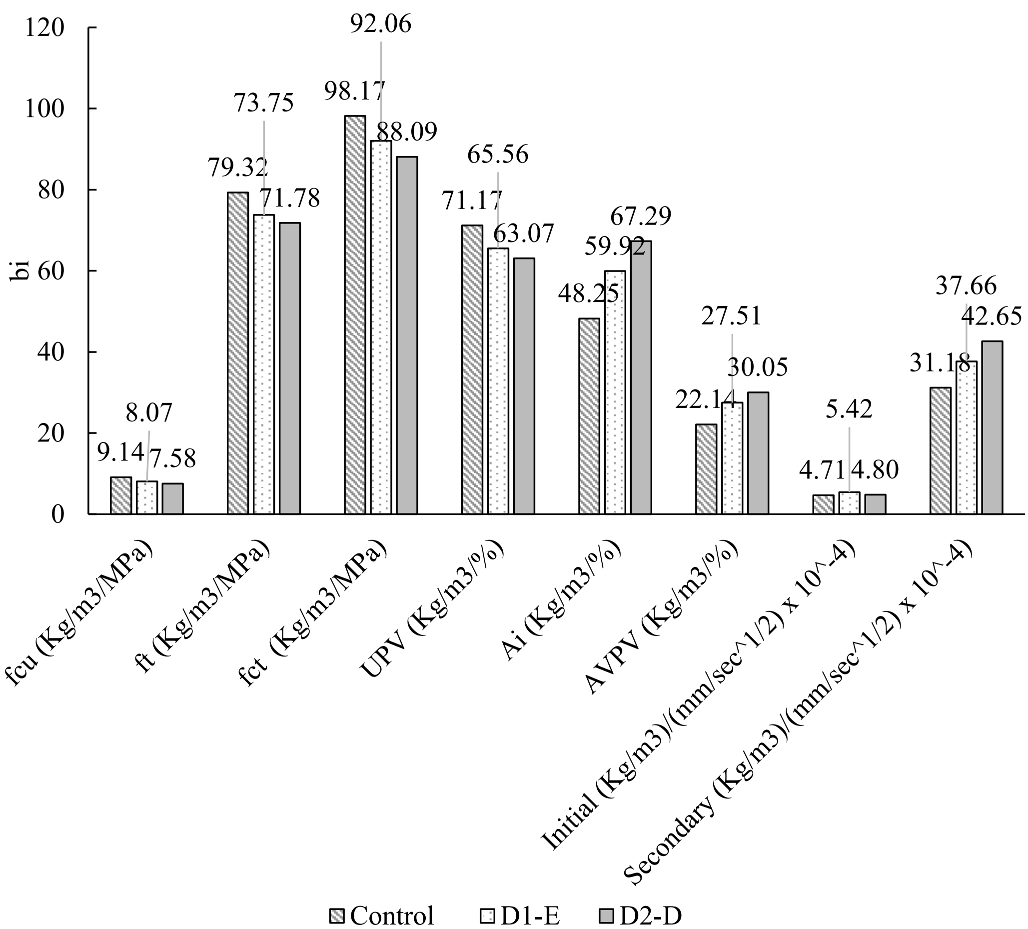

Fig. 19 Results of bi for control specimens, D1-F and D2-E at 28 days

3.5 Cement Consumption Reduction

The addition of GNP can enhance mechanical, homogeneity and water resistance of concrete specimens, thus resulting in reducing the amount of cement required to achieve a given strength class. In this study, the reduction of cement consumption was evaluated in terms of binder intensity (bi). The bi is an indicator which allowed the direct comparison of various concrete mix designs in terms of binder use. This indicator is used to measure the binder consumption needed to deliver one unit of functional performance measured by a relevant indicator. This relevant indicator can be, for example: compressive strength, flexural strength, elastic modulus, durability, and electrical or thermal performance. the bi is defined as the total amount of binder required to deliver one unit of functional performance measured by a relevant indicator at a given age (Damineli et al., 2010, 2013). For instance, in terms of compressive strength, the most common indicator used by construction industry and research community, bi is used to measure the amount of binder (Kg) required to provide 1 MPa. Bi is calculated using the following equation:

$$b_i = \frac{b}{p} \tag{4}$$

where:

b = total amount of cement required (Kg/m^3).

p = performance requirement.

The results of the bi for control concrete, D1-F and D2-E at 28 days are presented in Fig. 19. Regarding compressive strength, the bi of control concrete, D1-F and D2-E is 9.1, 8.1 and 7.6 kg $m^{-3}MPa^{-1}$. International benchmarks indicated that the bi of concrete with compressive strength between 20 and 40 MPa is between approximately 13 to 7 kg m^{-3} MPa^{-1} (Damineli et al., 2010, 2013). The results showed that the bi of all three concrete mixes were within the range indicated by international benchmarks. Moreover, when comparing binder consumption required for each concrete mix using bi,, it can be observed that for mixes D1-F and D2-E, the total amount of binder required to deliver 1 MPa can be reduced by up to 11.6% and 17.1%. This demonstrates that GNP can be used to produce concrete with lower binder consumption. Furthermore, apart from enhancing mechanical properties, GNP showed even greater benefits in improving water resistance of concrete. For instance, for D2-E the bi of Ai, AVPV, and initial and secondary sorptivity can be reduced by 39,4%, 35,8%, 28.3% and 36.8%, while for D1-F the bi was reduced by 24.2%, 24.3%, 13.7% and 20.8%. Therefore, the enhancement in water resistance leads to an increase in the durability of concrete. This, in turn, results in increasing the life cycle of concrete structures, thus causing a reduction of CO_2 emissions through a reduction in maintaining, repairing, and renovating the structure.

4 Conclusions

This study evaluated the effect of adding GNP dispersion prepared using two different dispersion techniques on the fresh, mechanical and durability performance of concrete. Based on the findings of this study, the following conclusions can be drawn:

- The addition of 0.25 wt% GNP generally reduces the slump values of fresh concrete mixes. Water molecules attach to the surface of GNP, resulting in a reduction in the available water required to maintain workability of fresh concrete mixes. The use of SP mitigates the adverse effect of GNP on the workability of fresh concrete mixes. Different optimum SP concentrations are found for non-sonicated (SP:0.9 wt%) and sonicated (SP:0.08 wt%) GNP dispersion. This difference may be due to the higher energy that is transferred by sonication to overcome the van der Waals force of attraction between the graphene layers compared to the low shear forces produce by the dill. Indeed, nanosheets are less likely to be exfoliated and de-aggregated in non-sonicated GNP dispersion than in sonicated dispersion. The agglomeration of nanosheets in the non-sonicated GNP dispersion alters the physical interaction between water and cement grains, reducing their chemical reaction, which in turn negatively affects the workability of concrete.
- The addition of sonicated GNP dispersion increases compressive, flexural and tensile strength by 20.8%, 10.5% and 11.4%, respectively. This may due to the reinforcement of microstructure of concrete by nucleation effect of cement hydration products on the surface of GNP which lead to the control of crack propagation, the increase in crack tortuosity, and the enhancement in stress distribution. In addition, non-sonicated GNP dispersion has a lower improvement in mechanical properties which may be due to agglomeration of nanosheets in non-sonicated GNP dispersion reduces the uniform distribution of GNP in the cement matrix causing a reduction in the control over the crack propagation and tortuosity, as well as the stress distribution produced by the nucleation effect of GNP.
- The water resistance and quality of concrete is improved by adding GNP. The sonicated GNP dispersion has the highest improvement in both water resistance and quality of concrete. Indeed, sonicated GNP dispersion increases UPV, Ai, AVPV, initial and secondary sorptivity by 12.9%, 28.3%, 19.5%, 22% and

27%, respectively. The increase in water resistance and quality of concrete may be due to GNP refine the pore structure of the concrete, leading to a more homogeneous and uniform material. This refinement of microstructure prevents the ingress of liquids into concrete and creates a more tortuous path for water to enter and move through concrete. As a result, concrete is more resistant to water and has a higher quality, thus improving its durability. Similar to mechanical properties, non-sonicated GNP dispersion has a lower impact on water resistance and quality of concrete, which may be due to the agglomeration of GNP in the cement matrix reduces their uniform distribution causing defects in the cement matrix. Thus, the nucleation sites for GNP precipitation and filling effect are reduced, affecting the porosity of concrete.

- The SEM images revealed that C–S–H products were formed at the interface with GNP. As C–S–H products precipitate on the surface of the GNP, they may grow in various directions, covering different areas of the surface of the nanosheets. This indicated that GNP may serve as nucleation sites for precipitating hydration cement products, thus strengthening the microstructure of the cement matrix and providing a more compact and homogeneous concrete, leading to improved mechanical and durability properties. A further analysis of the crack development in the surrounding of GNP shows that the nucleation effect of GNP can lead to improving mechanism of dissipation of energy, including crack deflection, branching and bridging, thus controlling the propagation and formation of micro-cracks.
- Concrete binder consumption decreased with the addition of GNP dispersion. The addition of sonicated GNP dispersion showed the highest reduction in binder consumption, which may be due to the agglomeration of GNP in non-sonicated dispersion. The shear forces produced by the drill are less efficient to overcome the van der Waals force of attraction between the graphene layers, thus achieving a lower level of exfoliation of nanosheets in non-sonicated GNP dispersion compared to the sonication GNP dispersion. Ultrasound energy creates local breaks of fluid-generating cavities, which, when collapsing, produce localized high-intensity jets responsible for the peeling of graphene layers from graphite, resulting in GNP dispersion with lower nanosheet agglomeration and a greater level of exfoliation. Therefore, the nanosheets in sonicated GNP dispersion are more uniformly distributed in the concrete, maximizing the nucleation effects and filling effects of GNP, thus leading to a higher reduction in binder consumption. For instance, in terms of compressive, flexural and tensile strength, the bi of D2-E was reduced by 17.1%, 9.5% and 10.3%, respectively. In addition, greater reduction in binder consumption is found in terms of water resistance of concrete. Indeed, the bi of Ai, AVPV, and initial and secondary sorptivity can be reduced by 39,4%, 35,8%, 28.3% and 36.8%, respectively. This indicated that an eco-friendlier concrete can be produced by adding GNP.

Abbreviations

Ai	Water absorption
AVPV	Apparent volume of permeable voids
CAC	Calcium aluminate cement
CCS	Carbon capture and storage
EDS	Energy dispersive spectrometry
FA	Fly ash
GO	Graphene oxide
GNP	Graphene nanoplatelets
GP	General purpose cement
GQDs	Graphene quantum dots
OPC	Ordinary Portland Cement
rGO	Reduced graphene oxide
RH	Relative humidity
SEM	Scanning electron microscopy
SP	Superplasticizer
UPV	Ultrasonic pulse velocity

Acknowledgements
The authors would like to Acknowledge Dr Dmitriy A. Dikin and Dr Sergey Voskresensky from APNTeK for the supply of the GNP material and their contributions to the preliminary stages of the project.

Author contributions
Dr Leidys Johana Jaramillo: Execution of experimental work, analysis of results and preparation of initial draft manuscript. A/Prof Robin Kalfat: The conception and design of the study, supervision, writing and revising the article critically for important intellectual content, final approval of the version to be submitted. All authors agree to be accountable for all aspects of the work.

Funding
No funding was received for this project.

Availability of Data and Materials
Data generated or analyzed during this study are available from the corresponding author upon reasonable request.

Declarations

Ethics approval and consent to participate
No ethics approval was required for this project.

Consent for publication
All authors hereby provide consent for the publication of the manuscript detailed above, including any accompanying images or data contained within the manuscript.

Competing interests
The authors declare that they have no known competing financial interests or personal relationships that could have appeared to influence the work reported in this paper.

Received: 28 May 2024 Accepted: 24 February 2025
Published online: 21 May 2025

References

Adhikary, S., Rudžionis, Ž., & Tučkutė, S. (2022). Characterization of aerogel and EGA-based lightweight cementitious composites incorporating different thickness of graphene platelets. *Journal of Building Engineering*. https://doi.org/10.1016/j.jobe.2022.104870

Ahmad, F., Jamal, A., Iqbal, M., Alqurashi, M., Almoshaogeh, M., Al-Ahmadi, H. M., & Hussein, E. E. (2022). Performance evaluation of cementitious composites incorporating nano graphite platelets as additive carbon material. *Materials*. https://doi.org/10.3390/ma15010290

Akaishi, A., Yonemaru, T., & Nakamura, J. (2017). Formation of water layers on graphene surfaces. *ACS Omega, 2*(5), 2184–2190.

Akono, A.-T. (2021). Fracture toughness of one- and two-dimensional nanoreinforced cement via scratch testing. *Philosophical Transactions of the Royal Society a: Mathematical, Physical and Engineering Sciences, 379*, 20200288.

Ali, M. B., Saidur, R., & Hossain, M. (2011). A review on emission analysis in cement industries. *Renewable and Sustainable Energy Reviews, 15*, 2252–2261.

Alwash, D., Kalfat, R., Du, H., & Al-Mahaidi, R. (2021). Development of a new nano modified cement based adhesive for FRP strengthened RC members. *Construction and Building Materials, 277*, 122318. https://doi.org/10.1016/j.conbuildmat.2021.122318

Andrew, R. M. (2019). Global CO2 emissions from cement production, 1928–2018. *Earth Syst. Sci. Data, 11*(4), 1675–1710.

Arslan, S., Öksüzer, N., & Gökçe, H. S. (2022). Improvement of mechanical and transport properties of reactive powder concrete using graphene nanoplatelet and waste glass aggregate. *Construction and Building Materials, 318*, 126199. https://doi.org/10.1016/j.conbuildmat.2021.126199

AS 1012.8. Compression and indirect tensile test specimens, Australian Standard (2014).

AS 1012.3.1. Determination of properties related to the consistency of concrete, Australian Standards (2014).

AS 1012.11. Methods of testing concrete Determination of the modulus of rupture, Standards Australia (2000).

AS 1012.10. Methods of testing concrete Method for the determination of indirect tensile strength of concrete cylinders ('Brazil' or splitting test), Standards Australia (2000).

AS 1012.21. Determination of water absorption and apparent volume of permeable voids in hardened concrete. Australian Standard: Australian (1999).

AS 3972, General purpose and blended cements, Standards Australia (2010)

ASTM C 1585.04. (2004) Standard test method for measurement of rate of absorption of water by hydraulic cement concretes. ASTM Standard American Society for Testing and Materials: USA.

ASTM C127–07, Standard Test Method For Density, Relative Density (Specific Gravity), And Absorption Of Coarse Aggregate, ASTM International (2007).

ASTM C128, Standard Test Method for Density, Relative Density (Specific Gravity), and Absorption of Fine Aggregate, ASTM International (2007).

ASTM C597. Standard test method for pulse velocity through concrete. ASTM Standard American Society for Testing and Materials: USA (2016).

Babak, F., Hassani, A., Rashidi, A., & Parviz, G. (2014). Preparation and mechanical properties of graphene oxide: Cement nanocomposites. *The Scientific World Journal, 2014*, 276323.

Bandilla, K. W. (2020). Carbon capture and storage. In T. M. Letcher (Ed.), *Future Energy* (pp. 669–692). Elsevier: Amsterdam.

Baomin, W., & Shuang, D. (2019). Effect and mechanism of graphene nanoplatelets on hydration reaction, mechanical properties and microstructure of cement composites. *Construction and Building Materials, 228*, 116720.

Barcelo, L., Kline, J., Walenta, G., & Gartner, E. (2014). Cement and carbon emissions. *Materials and Structures*. https://doi.org/10.1617/s11527-013-0114-5

Bentz D, Clifton JR, Ferraris CF, Garboczi EJ. (1999). Transport properties and durability of concrete: literature review and research plan.

Chen, G., Yang, M., Xu, L., Zhang, Y., & Wang, Y. (2019). Graphene nanoplatelets impact on concrete in improving freeze-thaw resistance. *Applied Sciences, 9*, 3582.

Chen, W., Xu, L., & Hua, Z. (2020). Mechanical properties and shrinkage behavior of concrete-containing graphene-oxide nanosheets. *Materials, 13*, 590.

Chen, Y., Li, G., Li, L., Zhang, W., & Dong, K. (2023). Molecular dynamics simulation and experimental study on mechanical properties and microstructure of cement-based composites enhanced by graphene oxide and graphene. *Molecular Simulation, 49*(3), 251–262. https://doi.org/10.1080/08927022.2022.2156560

Chen, Y.-H., Lin, S.-C., Wang, J.-A., Hsu, S.-Y., & Ma, C.-C. (2018). Preparation and properties of graphene/carbon nanotube hybrid reinforced mortar composites. *Magazine of Concrete Research, 71*, 1–37.

Dalla, P., Tragazikis, I., Trakakis, G., Galiotis, C., Dassios, K., & Matikas, T. (2021). Multifunctional cement mortars enhanced with graphene nanoplatelets and carbon nanotubes. *Sensors, 21*, 933.

Damineli, B. L., Kemeid, F. M., Aguiar, P. S., & John, V. M. (2010). Measuring the eco-efficiency of cement use. *Cement and Concrete Composites, 32*(8), 555–562.

Damineli, B. L., Pileggi, R. G., & John, V. M. (2013). 2 - Lower binder intensity eco-efficient concretes. In F. Pacheco-Torgal, S. Jalali, J. Labrincha, & V. M. John (Eds.), *eco-efficient concrete* (pp. 26–44). Woodhead Publishing: UK.

Dong, H., Gao, P., & Ye, G. (2017). Characterization and comparison of capillary pore structures of digital cement pastes. *Materials and Structures, 50*(2), 154.

Du, H., Gao, H., & Pang, S. (2016). Improvement in concrete resistance against water and chloride ingress by adding graphene nanoplatelet. *Cement and Concrete Research, 83*, 114–123.

Du, H., & Pang, S. (2015). Enhancement of barrier properties of cement mortar with graphene nanoplatelet. *Cement and Concrete Research*. https://doi.org/10.1016/j.cemconres.2015.05.007

Du, H., & Pang, S. (2018). Dispersion and stability of graphene nanoplatelet in water and its influence on cement composites. *Construction and Building Materials, 167*, 403–413.

Gallucci, E., & Scrivener, K. (2007). Crystallisation of calcium hydroxide in early age model and ordinary cementitious systems. *Cement and Concrete Research, 37*(4), 492–501.

Gjørv, O. (2011). Durability of concrete structures. *Arabian Journal for Science and Engineering - ARAB J SCI ENG, 36*, 151–172.

Han, S.-H., Park, W.-S., & Yang, E. I. (2013). Evaluation of concrete durability due to carbonation in harbor concrete structures. *Construction and Building Materials, 48*, 1045–1049.

Hanzic, L., & Ilic, R. (2003). Relationship between liquid sorptivity and capillarity in concrete. *Cement and Concrete Research*. https://doi.org/10.1016/S0008-8846(03)00070-X

Jaramillo, L. J., & Kalfat, R. (2023). Fresh and hardened performance of concrete enhanced with graphene nanoplatelets (GNP). *Journal of Building Engineering, 75*, 106945.

Jiang, Z., Sevim, O., & Ozbulut, O. (2021). Mechanical properties of graphene nanoplatelets-reinforced concrete prepared with different dispersion techniques. *Construction and Building Materials, 303*, 124472. https://doi.org/10.1016/j.conbuildmat.2021.124472

Jiang, Z., Sherif, M., Xing, G., & Ozbulut, O. (2020). Tensile characterization of graphene nanoplatelets (GNP) mortar using acoustic emissions. *Materials Today Communications, 25*, 101433. https://doi.org/10.1016/j.mtcomm.2020.101433

Lin, Y., & Du, H. (2020). Graphene reinforced cement composites: A review. *Construction and Building Materials, 265*, 120312.

Liu, Q., Xu, Q., Yu, Q., Gao, R., & Tong, T. (2016). Experimental investigation on mechanical and piezoresistive properties of cementitious materials containing graphene and graphene oxide nanoplatelets. *Construction and Building Materials*. https://doi.org/10.1016/j.conbuildmat.2016.10.024

Lovecchio, N., Shaikh, F., John, M., Ceravolo, R., & Biswas, W. (2020). Environmental assessment of supplementary cementitious materials and engineered nanomaterials concrete. *AIMS Environmental Science, 7*, 13–30.

Madlool, N., Rahman, S., Abd Rahim, N., & Kamalisarvestani, M. (2013). An overview of energy savings measures for cement industries. *Renewable and Sustainable Energy Reviews, 19*, 18–29.

Malhotra, V., & Carino, N. (2004). *The ultrasonic pulse velocity method*. London: CRC Handbook on Nondestructive Testing of Concrete.

Mohammed, B., Syed, Z., Khed, V., & Qasim, M. (2017). Evaluation of nano-silica modified ECC based on ultrasonic pulse velocity and rebound hammer, The Open Civil. *Engineering Journal, 11*, 638–649.

Papanikolaou, I., de Souza, L. R., Litina, C., & Al-Tabbaa, A. (2021a). Investigation of the dispersion of multi-layer graphene nanoplatelets in cement composites using different superplasticiser treatments. *Construction and Building Materials, 293*, 12.
Papanikolaou, I., Ribeiro de Souza, L., Litina, C., & Al-Tabbaa, A. (2021b). Investigation of the dispersion of multi-layer graphene nanoplatelets in cement composites using different superplasticiser treatments. *Construction and Building Materials, 293*, 123543.
Papayianni, I., & Anastasiou, E. (2010). Production of high-strength concrete using high volume of industrial by-products. *Construction and Building Materials, 24*, 1412–1417.
Polverino, S., Del Rio Castillo, A., Brencich, A., Marasco, L., Bonaccorso, F., & Morbiducci, R. (2022). Few-layers graphene-based cement mortars: production process and mechanical properties. *Sustainability*. https://doi.org/10.3390/su14020784
Rajesh, V., & Narendra Kumar, B. (2022). Influence of nano-structured graphene oxide on strength and performance characteristics of high strength fiber reinforced self compacting concrete. *Materials Today, 60*, 694–702.
Richardson, I. G. (1999). The nature of C-S-H in hardened cements. *Cement and Concrete Research, 29*(8), 1131–1147.
Safuta, M., Pakulski, D., Górski, M., Szojda, L., Ciesielski, A., & Samorì, P. (2021). Electrochemically exfoliated graphene for high-durability cement composites. *ACS Applied Materials & Interfaces*. https://doi.org/10.1021/acsami.1c04451
Sandhya, M., Devarajan, R., Kadirgama, K., & Harun, W. S. W. (2021). Ultrasonication an intensifying tool for preparation of stable nanofluids and study the time influence on distinct properties of Graphene Nanofluids - A systematic overview. *Ultrasonics Sonochemistry, 73*, 105479.
Shuang, D., Hongmei, A., & Baomin, W. (2022). Research on the electromagnetic wave absorption properties of GNP/EMD cement composite. *Construction and Building Materials, 321*, 126398. https://doi.org/10.1016/j.conbuildmat.2022.126398
Simpkins, J. E., Strehlow, R. A., Mioduszewski, P. K., & Uckan, T. (1989). Control of water absorption by purification of graphite. *Journal of Nuclear Materials, 162–164*, 871–875.
Souza, F., Yao, X., Lin, J., Naseem, Z., Tang, Z., Hu, Y., Gao, W., Sagoe-Crentsil, K., & Duan, W. (2022). Effective strategies to realize high-performance graphene-reinforced cement composites. *Construction and Building Materials, 324*, 126636.
Taylor, H. F. (1997). *Cement chemistry*. Thomas Telford London: UK.
Tong, T., Fan, Z., Liu, Q., Wang, S., Tan, S., & Yu, Q. (2016). Investigation of the effects of graphene and graphene oxide nanoplatelets on the micro- and macro-properties of cementitious materials. *Construction and Building Materials, 106*, 102–114.
VicRoads Technical note 89, Test methods for the assessment of durability of concrete, VicRoads, (2007).
Wang, B., Jiang, R., & Wu, Z. (2016). Investigation of the mechanical properties and microstructure of graphene nanoplatelet-cement composite. *Nanomaterials, 6*, 200.
Wang, B., & Pang, B. (2019). Mechanical property and toughening mechanism of water reducing agents modified graphene nanoplatelets reinforced cement composites. *Construction and Building Materials, 226*, 699–711.
Wang, B., & Shuang, D. (2018). Effect of graphene nanoplatelets on the properties, pore structure and microstructure of cement composites. *Materials Express, 8*, 407–416.
Wang, B., & Zhao, R. (2017). Effect of graphene nano-sheets on the chloride penetration and microstructure of the cement based composite. *Construction and Building Materials*. https://doi.org/10.1016/j.conbuildmat.2017.12.094
Whitehurst, E. A. (1951). Soniscope tests concrete structures. *ACI Journal Proceedings, 47*, 2.
Win, T. T., Prasittisopin, L., Jongvivatsakul, P., et al. (2023). Investigating the synergistic effect of graphene nanoplatelets and fly ash on the mechanical properties and microstructure of calcium aluminate cement composites. *J. Build. Eng., 78*, 107710.
Win, T. T., Prasittisopin, L., Nganglumpoon, R., Pinthong, P., Watmanee, S., Tolek, W., & Panpranot, J. (2024a). Innovative GQDs and supra-GQDs assemblies for developing high strength and conductive cement composites. *Construction and Building Materials, 421*, 135693.
Win, T. T., Prasittisopin, L., Nganglumpoon, R., Pinthong, P., Watmanee, S., Tolek, W., & Panpranot, J. (2024b). Chemo-physical mechanisms of high-strength cement composites with suprastructure of graphene quantum dots. *Cleaner Materials, 11*, 100229.
Wu, S., Qureshi, T., & Wang, G. (2021). Application of graphene in fiber-reinforced cementitious composites: A review. *Energies, 14*, 4614.
Xu, Y., Cao, H., Xue, Y., Li, B., & Cai, W.-H. (2018). Liquid-phase exfoliation of graphene: An overview on exfoliation media, techniques, and challenges. *Nanomaterials, 8*, 942.
Zeng, H., Lai, Y., Qu, S., & Yu, F. (2021). Effect of graphene oxide on permeability of cement materials: An experimental and theoretical perspective. *Journal of Building Engineering, 41*, 102326.

Publisher's Note

Leidys Johana Jaramillo is a structural engineer who completed her PhD at Swinburne University of Technology. Her research interests include the development of environmentally sustainable concrete using graphene nano platelets, sustainable construction materials and the durability of concrete structures.

Robin Kalfat is currently appointed as an Associate Professor of Structural Engineering at Swinburne University of Technology. His research interests include: strengthening and rehabilitation of structures, sustainable construction materials, fire performance of FRP strengthened structures, the use of nano materials such as graphene to improve the strength and durability of concrete and advanced numerical techniques for structural analysis.